Redox Biology 34 (2020) 101542

Contents lists available at ScienceDirect

Redox Biology

journal homepage: www.elsevier.com/locate/redox

# MnTE-2-PyP, a manganese porphyrin, reduces cytotoxicity caused by irradiation in a diabetic environment through the induction of endogenous antioxidant defenses

Arpita Chatterjee[a], Elizabeth A. Kosmacek[a], Shashank Shrishrimal[a], J. Tyson McDonald[b], Rebecca E. Oberley-Deegan[a,*]

[a] Department of Biochemistry and Molecular Biology, University of Nebraska Medical Center, Omaha, NE, USA
[b] Department of Physics & Cancer Research Center, Hampton University, Hampton, VA, 23668, USA

ARTICLE INFO

*Keywords:*
Radiation
Diabetes
Manganese porphyrin
ROS
NRF2
Hyperglycemia

ABSTRACT

Radiation is a common anticancer therapy for many cancer patients, including prostate cancer. Diabetic prostate cancer patients suffer from increased lymph node metastasis, tumor recurrence and decreased survival as compared to non-diabetic prostate cancer patients. These patients are also at increased risk for enhanced radiation-induced normal tissue damage such as proctitis. Diabetics are oxidatively stressed and radiation causes additional oxidative damage. We and others have reported that, MnTE-2-PyP, a manganese porphyrin, protects normal prostate tissue from radiation damage. We have also reported that, in an *in vivo* mouse model of prostate cancer, MnTE-2-PyP decreases tumor volume and increases survival of the mice. In addition, MnTE-2-PyP has also been shown to reduce blood glucose and inhibits pro-fibrotic signaling in a diabetic model. Therefore, to investigate the role of MnTE-2-PyP in normal tissue protection in an irradiated diabetic environment, we have treated human prostate fibroblast cells with MnTE-2-PyP in an irradiated hyperglycemic environment. This study revealed that hyperglycemia causes increased cell death after radiation as compared to normo-glycemia. MnTE-2-PyP protects against hyperglycemia-induced cell death after radiation. MnTE-2-PyP decreases expression of NOX4 and α-SMA, one of the major oxidative enzymes and pro-fibrotic molecules respectively. MnTE-2-PyP obstructs NF-κB activity by decreasing DNA binding of the p50-p50 homodimer in the irradiated hyperglycemic environment. MnTE-2-PyP increases NRF2 mediated cytoprotection by increasing NRF2 protein expression and DNA binding. Therefore, we are proposing that, MnTE-2-PyP protects fibroblasts from irradiation and hyperglycemia damage by enhancing the NRF2- mediated pathway in diabetic prostate cancer patients, undergoing radiotherapy.

## 1. Introduction

It is reported that 8%–18% of all cancer patients have pre-existing diabetes and diabetic cancer patients have a 42% increased mortality rate and a 21% increased rate of tumor recurrence as compared to non-diabetic patients [1,2]. Although the occurrence of prostate cancer may be lower compared to other cancers among diabetic individuals, prostate cancer patients with diabetes have more than a thirty percent increase in mortality as compared to non-diabetic prostate cancer patients [3,4]. Hyperglycemia is also responsible for increased growth of prostate tumors [5]. Due to altered insulin/IGF-1 signaling, diabetic prostate cancer patients have elevated androgen receptor signaling, which itself increases androgen dependent growth and also causes failure of androgen deprivation therapy [6]. Diabetic prostate cancer patients also have significantly increased risk of lymph node metastasis [7]. Radiation therapy is one of the major anti-cancer therapies for prostate cancer. Diabetic prostate cancer patients suffer from increased failure to control tumor growth with radiotherapy. Diabetics are also more prone to radiation damage. Specifically, diabetics have significantly higher incidence of radiation-induced proctitis and gastrointestinal and genitourinary complications as compared to non-diabetic prostate cancer patients [8–10]. Radiation-induced acute side effects can be so severe that radiation therapy has to be halted, which leads to suboptimal treatment of the tumor, reduced quality of life and early death. To date, there are no radioprotectors used clinically to protect diabetic normal tissues from radiation damage.

* Corresponding author. Department of Biochemistry and Molecular Biology, 985870# BCC 6Nebraska Medical Center Omaha, NE, 68106, USA.
*E-mail address:* becky.deegan@unmc.edu (R.E. Oberley-Deegan).

https://doi.org/10.1016/j.redox.2020.101542
Received 4 March 2020; Received in revised form 3 April 2020; Accepted 13 April 2020
Available online 21 April 2020

Major antidiabetic agents in clinics are insulin and metformin. Diabetic prostate cancer patients taking insulin experience increased toxicity and inferior outcomes after radiotherapy [11]. Although metformin has shown some protective effects on normal tissue after radiotherapy [12,13], there were no survival benefits reported after use of metformin [14]. In a hyperglycemic environment it is also reported that, metformin is unable to inhibit the growth of PC-3 cells, an aggressive prostate cancer cell [15]. Therefore, to achieve better treatment outcomes and quality of life, diabetic prostate cancer patients who are undergoing radiotherapy need additional therapy, which will protect from radiation-mediated normal tissue damage and promote the anti-cancer effect of radiation to reduce clinical complications.

Radiation is recognized as a classic model of oxidant radical production, a property exploited for cancer cell killing, but also results in the damage of normal tissues. Diabetics are oxidatively stressed due to high levels of reactive oxygen species (ROS) from oxidases and mitochondrial leakage [16–19]. Due to already elevated ROS, when diabetic cancer patients undergo radiation therapy, they are more prone to radiation mediated normal tissue damage as compared to non-diabetics. Therefore, suppression of ROS generated by hyperglycemia and irradiation can be a fruitful therapeutic strategy to protect normal tissue damage in diabetic prostate cancer patients.

MnTE-2-PyP is a ROS scavenger and potent radioprotector that reduces normal tissue fibrosis through the scavenging of superoxide and inhibition of NADPH oxidase 4 (NOX4)-TGFβ signaling in irradiated normal tissues and cells, including prostate fibroblasts [20–23]. It is previously reported that in macrophages, MnTE-2-PyP is present in both the nucleus and cytosol [24]. We and others have also shown that, MnTE-2-PyP does not obstruct radiation mediated cancer cell death. Rather, it enhances radiation mediated prostate tumor reduction in *in vivo* models [25]. In the context of diabetes, MnTE-2-PyP protects from high glucose-induced pancreatic β cell apoptosis, enhances glucose absorption rate, decreases insulin resistance and reduces NF-κB mediated pro-inflammatory signaling [26,27]. MnTE-2-PyP also inhibits the expression of PAI-1, a crucial player in tissue fibrosis and cardiovascular disease in diabetics [28]. Taken together, we hypothesize that MnTE-2-PyP has the potential to significantly reduce hyperglycemia and radiation-induced damage of normal tissues in a diabetic irradiated environment.

To mimic a diabetic irradiated environment, we have irradiated (3 Gy of X-rays) human prostate fibroblast cells in a hyperglycemic environment (20 mM glucose) in the presence or absence of MnTE-2-PyP. This study revealed that MnTE-2-PyP protected from irradiation and hyperglycemia-induced cell death and suppressed NOX4 and α-SMA expression, two major regulators of pro-fibrotic signaling. In addition, MnTE-2-PyP reduced the DNA binding of NF-κB, a major pro-inflammatory molecule, in irradiated hyperglycemic cells. MnTE-2-PyP enhanced the cytoprotective antioxidant signaling by enhancing NRF2 expression and activity.

Radiation and high glucose-induced cellular damage is caused by inflammation and dysfunctional antioxidant signaling, which leads to fibrosis. This is the first study to demonstrate that MnTE-2-PyP treatment can reduce all of these damaging pathways and protect the normal fibroblast cells during irradiation in a hyperglycemic environment. This study intensely advocates that diabetic cancer patients need more therapeutic care as compared to non-diabetics for reducing radiation-mediated complications and that MnTE-2-PyP would be an excellent agent for enhancing the quality of life of these patients after radiation.

## 2. Materials and methods

### 2.1. Cell culture and treatment conditions

P3158 cells were used for every experiment in this study. P3158 cells are cultured from primary prostate tissue collected from the prostate of a heathy male and immortalized using a pBABE-hygro-hTERT plasmid (Addgene, plasmid #1773) and the immortalized cells were obtained from Dr. McDonald J. Tyson. P3158 cells were cultured in RPMI-1640 (Hyclone, catalog number: SH30027.01) media, supplemented with 10% fetal bovine serum (FBS) and 1% penicillin/streptomycin. This media contains 11.1 mM glucose, or 200 mg/dL. Cells cultured in this media are referred to as control or normo-glycemic condition in this study. For mimicking hyperglycemia in diabetes, we have added an extra 20 mM glucose in the media, which corresponds to 360 mg/dL, for a total of 559.8 mg/dL. This condition is referred as the high glucose (HG) condition in this study. P3158 cells were seeded with 20 mM glucose (for HG) and/or 30 μM Manganese (III) Meso-Tetrakis-(*N*-ethylpyridinium-2-yl) (referred as MnTE-2-PyP or T2E), which was a kind gift from Dr. James Crapo, National Jewish Health, Denver, CO. Twenty four hours later, half of the cells were irradiated with 3 Gy of X-rays using the Rad Source RS-2000 (referred as RAD). Then the cells were incubated in 37 °C in a 5% $CO_2$ environment. Unless otherwise indicated, on the fifth day after radiation, cells were harvested for all the assays. If not otherwise specified, we had eight groups for each study- 1. Control, 2. HG, 3.T2E, 4. HG + T2E, 5. RAD, 6. RAD + HG, 7. RAD + T2E and 8. RAD + HG + T2E.

### 2.2. Cell viability measurement

Trypan blue exclusion method was used to determine the number of viable cells. In brief, $1 \times 10^5$ cells were seeded for each experimental condition either with HG, 20 mM mannitol (as an osmolality control for 20 mM glucose), RAD, T2E or in combinations. On the fifth day post-radiation, cells were trypsinized, pelleted and 1 mL of media was used to resuspend the cells. Cells were then mixed with trypan blue at a 1:1 ratio and loaded in a cell counting chamber slide and enumerated with a Countess II cell counter (Life Technologies). The number and percentage of live, dead and total cells were calculated.

### 2.3. Quantitative real time PCR

Five days after radiation, total RNA was isolated using a Quick-RNA™ MiniPrep (cat #R1055) kit by Zymo Research following the manufacture's protocol. Infinite M200Pro plate reader (Tecan) was used to measure the concentration and quality of RNA. Total RNAs having a 260/280 ratio ~2.0 were used for further experiments. RNA (40 ng) was used to amplify NOX2 and NOX4 transcripts using Power SYBR Green RNA-to-$C_t$ kit (Applied Biosystem, part number: 4389986). The same amount of RNA was used to study the expression of 18S rRNA gene as an internal control using manually designed primers. All PCR experiments were performed in a Bio-Rad CFX96 real time thermal cycler. The primer sequences for NOX2 transcript were-forward: 5′-GTGCACAGCAAAGTGATTGG-3′ and reverse: 5′-GGCTTCCTCAGCTAC AACATCT-3′. The primer sequences for NOX4 transcript were-forward: 5′-AACACCTCTGCCTGTTCATC-3′ and reverse: 5′-GATACTCTGGCCCT TGGTTATAC-3′.

### 2.4. Western blot

$1.5 \times 10^6$ cells/T75 flask were seeded. After 24 h, cells were either sham irradiated or exposed to 3 Gy of radiation. Five days later, the cells were collected and used for preparing whole cell, nuclear, cytosolic or mitochondrial extracts. For whole cell extract preparation, cell pellets were lysed using a cell lysis buffer [120 mM NaCl, 50 mM Tris-HCl, 5 mM EDTA, 1% NP-40 and complete protease inhibitor cocktail tablets (Roche, cat # 11697498001; 1 tablet/50 ml)]. After incubation for 30 min on ice, cell lysates were sonicated with 8 pulses at 40% amplitude. After sonication, lysates were centrifuged at 4°C for 15 min at 15,000g and supernatants were collected. CelLytic NuCLEAR Extraction kit (Sigma Aldrich, NXTRACT-1KT) was used for preparing nuclear and cytosolic extracts. For mitochondrial extract preparation, Mitochondria Isolation Kit for Mammalian Cells (Thermo Scientific,

reference number: 89874) was used. All the protein extracts were assayed for total protein concentrations by a Bradford reagent (Amresco) using bovine serum albumin as a standard. Proteins were loaded on to Bolt 4–12% Bis-Tris Plus gels (Thermo Fisher Scientific) and transferred to nitrocellulose membranes (Life Technologies). After incubation with 5% nonfat milk in TBST (10 mM Tris, pH 8.0, 150 mM NaCl, 0.5% Tween 20) for 2 h, the membranes were incubated with primary antibodies overnight. Membranes were then washed with TBST and incubated with a 1:10,000 dilution of HRP-conjugated secondary antibodies for 1–2 h at room temperature. Blots were then washed with TBST and developed with an ECL detection system (Thermo Fisher Scientific) and exposed to film. Films were scanned and the densitometry analyses of the scanned images were performed using ImageJ. Ponceau stained total protein was used as the loading control for each blot. Primary and secondary antibodies used in this study are listed as follows. α-SMA (Abcam, cat # ab5694, 1:3000 dilution), NOX1 (Abcam, cat # ab55831, 1:1000 dilution), NOX4 (Abcam, cat # ab133303, 1:1000 dilution), NOX2 (Abcam, cat # ab129068, 1:2000 dilution), Thioredoxin (Abcam, cat # ab26320, 1:2000 dilution), NFκB (Santa Cruz biotechnology, cat # sc-372, 1:500 dilution), NRF2 (Abcam, cat # ab62352, 1:1000 dilution), NQO1 (Novus biologicals, cat # NB200-209, 1:1000 dilution), TOMM20 (Abcam, cat # ab56783, 1:1000 dilution), Histone1 (Abcam, cat # ab125027, 1:1000 dilution), GAPDH (Cell Signaling Technology, cat # 2118S, 1:1000 dilution). Secondary goat anti-rabbit antibody (Invitrogen, reference number: A24537) and secondary goat-anti mouse antibody (Invitrogen, reference number: A24524) were used.

### 2.5. Superoxide measurement

In order to measure overall superoxide production in the cell, $1.5 \times 10^6$ cells/T75 flask were seeded with HG and T2E as described before. After 24 h, cells were either sham irradiated or radiated with 3 Gy of X-rays. Five days after radiation, the cells were harvested. After staining with 10 μM Dihydroethidium (DHE), cells were subjected to flow cytometric analysis using LSRII Green 532 Flow Cytometer (BD Biosciences). To specifically measure superoxide, 405/570 nm excitation/emission wavelengths were used. FACSDiVa analysis software (BD Biosciences) were used to analyze the data.

### 2.6. Nuclear ROS measurement

To measure the nuclear ROS, P3158 cells were seeded at a concentration of $1 \times 10^5$ cells/well on the coverslip in one well of a 6 well plate with HG and T2E as described before. After 24 h, cells were either sham irradiated or irradiated with 3 Gy of X-rays. Five days after radiation, the cells were washed with PBS and then stained with 10 μM of DHE (Invitrogen, D11347) for 15 min at 37°C in the dark. After incubation, the cells were washed in HBSS once and the coverslips were mounted on a slide with DAPI and immediately imaged with a Zeiss 710 Confocal Laser Scanning Microscope. In order to measure ROS products, 488/540 nm excitation/emission wavelengths were used. The images were analyzed using ImageJ. DAPI stained nuclear areas were marked and the mean florescence DHE intensity were measured only in those areas.

### 2.7. Electrophoretic mobility shift assay (EMSA)

For studying the DNA binding activity of NF-κB, NRF2, AP-1 and AP-2, $1.5 \times 10^6$ P3158 cells were seeded and irradiated as described before. Five days after radiation, nuclear protein extracts were harvested. Nuclear protein (10 μg) was used for each DNA binding assay (Promega Gel Shift Assay Core System, Cat# E3050). For NF-κB, AP-1 and AP-2 we used the consensus oligonucleotide from Promega (NFκB Cat# E329B, AP-1 Cat# E320B, AP2 Cat# E321B). For NRF2 consensus oligonucleotide, we have used NF-E2 Gel Shift Oligonucleotides from Santa Cruz Biotechnology (Cat# sc-2527). In brief, for each reaction, 35 pmole of each consensus oligonucleotide were labelled with $^{32}$P-ATP by T4 polynucleotide kinase according to the Promega protocol. After purification of labelled consensus oligonucleotides, 10 μg of nuclear protein were incubated with the oligonucleotides and electrophoresed in a 6% TBE gel (Life Technologies, cat # EC6265BOX) according to the Promega gel shift assay system protocol. Then the gel was air dried overnight using a Model 583 gel dryer backing cellophane (BIO-RAD, cat # 1650963) and a gel drying cassette. The dried gels with the cellophane were then exposed to film. Films were scanned and the densitometry analyses of the scanned images were performed using ImageJ.

### 2.8. NOX2 level measurement after proteasome inhibition

P3158 cells were seeded with HG and T2E as described above. Twenty four hours after seeding, cells were treated with 0.5 μM MG132 or equal volume of DMSO. After 30 min of MG132 treatment, cells were either sham irradiated or irradiated by 3 Gy of X-rays. Then the cells were incubated for five days. Then whole cell extract were prepared and subjected to western blot analysis for NOX2 as described above.

### 2.9. Thioredoxin (Trx) redox western blot

$1 \times 10^6$ cells/T75 flask were seeded. After 24 h, cells were either sham irradiated or exposed to 3 Gy of radiation. Five days later, the cells were collected and lysed with hypotonic lysis buffer (Sigma Aldrich, NXTRACT-1KT) in the presence of 50 mM iodoacetic acid. After centrifugation, the nuclear pellet was collected and lysed with G-lysis buffer (6 M Guanidine –HCl, 3 mM EDTA, 50 mM Tris-Cl, 0.5% Triton X-100, pH adjusted to 8.3 with NaOH) in the presence of protease inhibitor cocktail and 50 mM of iodoacetic acid. Samples were then purified using a G-25 column (GE healthcare, Life science). Two different flasks of cells were used as oxidation and reduction controls by treating with 5 mM $H_2O_2$ or 5 mM DTT respectively for 20 min prior to cell collection. Protein (50 μg) was run on a 20% native polyacrylamide gel for 90 min and transferred by a semi-dry transfer system (Life Technologies). Then redox isoforms of Trx was visualized by Trx antibody (Abcam, cat # ab26320, 1:2000 dilution) and HRP-conjugated secondary antibody. Blots were then developed with an ECL detection system as described above in the western blot section.

### 2.10. NRF2 knockdown by siRNA treatment

In one well of a 6 well plate, 75,000 cells were seeded with 25 nM control siRNA (Ambion, cat # 4390843) or NRF2 siRNA (Ambion, cat# 4392420). Twenty four hours later, HG and T2E were added in respective wells and incubated for another 24 h followed by radiation (3 Gy). Four days post-radiation, cells were harvested and whole cell lysates were prepared for western blot analysis.

### 2.11. Immunofluorescence assay

After treatment with HG, T2E and RAD, cells were incubated for five days after radiation, as indicated in the previous section. Then the cells were washed with PBS once and fixed by formalin for 10 min. After fixation, cells were washed thrice with PBS and permeabilized with 0.5% Triton X in PBS for 8 min. The cells were washed with PBS and blocked by 5% goat serum in PBS for 1 h. Cells were then incubated with a primary antibody for 2 h at room temperature followed by washing with PBS. Cells were incubated with florescence tagged secondary antibodies for 1 h. Finally cells were washed with PBS, mounted with a coverslip by ProLong Gold anti-fade reagent with DAPI (Invitrogen, cat #P36931) and imaged.

Antibodies used for these experiments are: NRF2 (Abcam, cat # ab ab62352, 1:2000 dilution) and Alexa fluor 488 goat-anti rabbit florescence secondary antibody (Life Technologies # A11008, 1:500

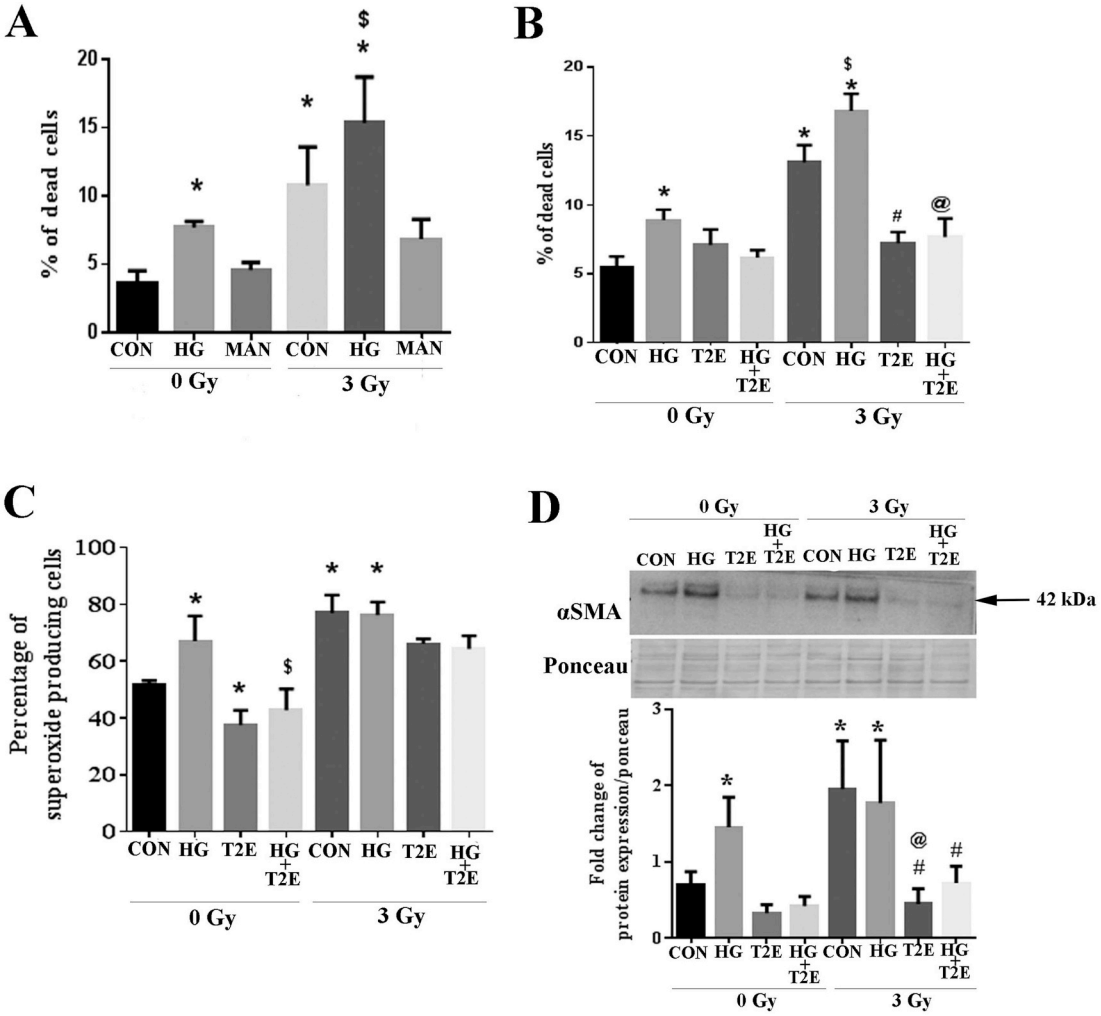


**Fig. 1. MnTE-2-PyP protected from radiation and hyperglycemia-induced normal cell death, oxidative stress and pro-fibrotic signaling.** Human prostate fibroblast cells were treated with 20 mM glucose (HG) or 20 mM mannitol (MAN) and/or 30 μM MnTE-2-PyP (T2E) followed by 3 Gy of X-rays (RAD). **A.** Percentage of fibroblast cell death. HG alone, RAD alone and the combination of HG and RAD significantly increased cell death as compared to control. Mannitol did not induce any significant cell death. **B.** Percentage of fibroblast cell death. T2E (30 μM) significantly decreased cell death in the irradiated group both in the presence and absence of HG as compared to PBS treated irradiated cells. **C.** The percentage of superoxide producing cells. Superoxide was significantly increased in HG, RAD and RAD + HG groups as compared to control. T2E treatment significantly reduced superoxide production. **D.** α-SMA protein expression. α-SMA was significantly increased in HG, RAD and RAD + HG groups as compared to control. T2E treatment significantly reduced α-SMA expression in HG, RAD and RAD + HG groups. n ≥ 3. (*) denotes a significant difference as compared to control, ($) denotes a significant difference as compared to HG, (#) denotes a significant difference as compared to RAD and (@) denotes a significant difference as compared to RAD + HG group.

dilution).

### 2.12. Measurement of prostate cancer cell death induced by conditioned media from human prostate fibroblast cells

We have selected PC-3 cells as a representative of advanced neuroendocrine type prostate cancer and LNCaP cells as a representative of early androgen sensitive prostate cancer. To study the role of HG, RAD and T2E treated fibroblasts on prostate cancer cell death, PC-3 and LNCaP cells were treated with conditioned media from HG, RAD and T2E treated human prostate fibroblast (P3158) cells. In brief, P3158 cells were seeded and treated with HG, T2E and RAD as mentioned above. Five days post-radiation, the conditioned media from P3158 cells were collected and centrifuged to spin down any cells. Then 3 mL of the conditioned media was added to the PC-3 or LNCaP cells, which were seeded (24 h before addition of conditioned media) in 6 well plates at $1 \times 10^5$ cells/well seeding density, in 3 mL of normal growth media (for PC-3: RPMI-1640, 10% FBS and 1% penicillin/streptomycin; for LNCaP: RPMI-1640, 5% FBS and 1% penicillin/streptomycin). Therefore, the final conditioned media concentration was 50%. As internal control conditions, PC-3 and LNCaP cells were cultured in their respective normal media, media with 20 mM glucose and in their respective conditioned media as well. Then PC-3 and the LNCaP cells were incubated for 4 days at 37°C in 5% $CO_2$ and collected for counting. A trypan blue assay was used to measure cell viability as previously discussed in the Cell Viability Measurement section.

### 2.13. Measurement of prostate cancer cell death in irradiated hyperglycemic condition

In 6 well plates, PC-3 and LNCaP cells ($1 \times 10^5$ cells/well) were cultured in their respective normal media, media with 20 mM glucose in the presence or absence of MnTE-2-PyP (30 μM). After 24 h of seeding, the cells were either sham irradiated or irradiated with 3 Gy of X-rays. Four days after radiation, a trypan blue assay was used to measure cell viability, as previously discussed in the Cell Viability Measurement section.

### 2.14. Statistical analyses

GraphPad Prism 6 Software version 6.0.5 for windows was used for all the statistical analyses. Unless otherwise indicated, values are the mean and standard deviation from three or more independent experiments. A statistically significant difference was determined by unpaired two-tailed *t*-test between two groups and one way ANOVA followed by post hoc Tukey's test were used for multiple comparisons.

## 3. Results

1. MnTE-2-PyP protected against radiation and hyperglycemia-induced normal cell death, oxidative stress and pro-fibrotic signaling

First, effects of hyperglycemia and radiation on fibroblast cell death were measured. In this study, 20 mM glucose was used to induce hyperglycemia and cells were irradiated with 3 Gy of X-rays. Patients often receive 2–3 Gy of irradiation for cancer therapy. In a previous study, we showed that 3 Gy radiation activates the human prostate fibroblasts (P3158) and decreased NRF2 signaling, which was recovered by MnTE-2-PyP in a normo-glycemic environment [23]. Therefore, to investigate the molecular mechanism of prostate fibroblast activation in irradiated hyperglycemia; we continued to use 3 Gy of radiation for this study.

There is a large range (5.5 mM–75 mM, or 99 mg/dL −1350 mg/dL) of glucose concentrations reported in the literature including, 20 mM, that were added to the basal glucose levels of the media to induce hyperglycemic stress in fibroblasts [29–33]. We have used 20 mM, which corresponds to 360 mg/dL of glucose, because it was a sub lethal dose for the fibroblasts but induced hyperglycemic stress. A blood glucose greater than 200 mg/dL is considered diabetic, so the 360 mg/dL of glucose reflects uncontrolled blood glucose levels. We wanted a model of hyperglycemic stress to determine the role of MnTE-2-PyP in regulating this condition.

In Fig. 1A, high glucose alone, radiation alone, or the combination of radiation and high glucose significantly increased death of the human prostate fibroblast cells as compared to control cells. The combination of radiation and high glucose also caused significantly higher cell death as compared to high glucose only treated cells. To confirm that the cytotoxic effect of high glucose was not due to the increased osmotic pressure in the media, cells were treated with 20 mM mannitol as a control. Mannitol has a comparable molecular weight of glucose and elicits similar osmotic changes as compared to glucose. Mannitol did not cause cell death in the presence or absence of radiation, indicating that the effects of high glucose were not due to osmotic changes (Fig. 1A).

We have previously published that MnTE-2-PyP (T2E) is a potent radioprotector, but we wanted to determine whether this compound could be beneficial in preventing radiation damage in a hyperglycemic environment. High glucose alone, radiation alone and the combination of high glucose and radiation exposure significantly increased cell death as compared to control and MnTE-2-PyP (30 μM) significantly decreased the cell death (Fig. 1B). Therefore, MnTE-2-PyP protects from radiation-induced cell death in a hyperglycemic environment.

We have also published that MnTE-2-PyP reduces superoxide production after radiation [20]. Radiation and hyperglycemia are both potent oxidative stressors. Therefore, we tested the overall superoxide scavenging capacity of MnTE-2-PyP in irradiated, hyperglycemic cells. High glucose alone, radiation alone and the combination of high glucose and radiation exposure significantly enhanced the percentage of overall superoxide producing cells as compared to control. MnTE-2-PyP (30 μM) decreased superoxide production in irradiated cells, significantly in the high glucose treated cells (Fig. 1C). Therefore, MnTE-2-PyP protects from overall oxidative stress in a hyperglycemic environment.

Alpha-smooth muscle actin (α-SMA) is a major pro-fibrotic molecule and is downstream of the TGFβ/NOX4 pro-fibrotic signaling pathway. Normal fibroblasts express basal levels of α-SMA but when fibroblasts become activated, these cells express significantly more α-SMA. These activated fibroblasts are thought to be responsible for laying down aberrant extracellular matrix leading to fibrosis. There was a significant increase in α-SMA in cells treated with high glucose alone, radiation alone or the combination of radiation and high glucose as compared to control cells. The addition of MnTE-2-PyP significantly inhibited α-SMA expression in the cells treated with high glucose or radiation alone or in combination (Fig. 1D). Thus, MnTE-2-PyP significantly decreased α-SMA expression in irradiated normal prostate fibroblast cells exposed to hyperglycemia, indicating that MnTE-2-PyP treatment inhibits fibroblast activation even in an irradiated high glucose environment.

2. MnTE-2-PyP inhibited NOX4 expression and restored NOX2 expression after radiation

As high glucose and radiation-induced superoxide levels were reduced by MnTE-2-PyP, we next investigated the expression level of NOX enzyme proteins. NOX1 protein level was not altered in any of our experimental conditions (Supplementary Fig. 1A). NOX4 is one of the major ROS producing NOX enzymes in response to radiation. NOX4 has also been shown to regulate α-SMA levels in fibroblasts in response to TGF-β stimulation [34]. Therefore, NOX4 expression levels were investigated in human prostate fibroblasts in normo-glycemic or hyperglycemic conditions in the presence or absence of irradiation. Our study revealed that high glucose alone, radiation alone, or the combination of high glucose and radiation, significantly increased NOX4 mRNA levels as compared to controls (Fig. 2A). NOX4 mRNA expression was also significantly increased in the combination group (radiation and high glucose) as compared to high glucose or radiation only groups. Conversely, MnTE-2-PyP treatment significantly decreased NOX4 mRNA expression in all conditions tested (Fig. 2A).

Interestingly, NOX4 protein levels did not follow the NOX4 mRNA expression. Radiation alone was the only condition that significantly elevated NOX4 protein levels and this was only a 2 fold induction (Fig. 2B). The combination of radiation and high glucose produced only slightly elevated NOX4 protein levels, which was not significant. However, the addition of MnTE-2-PyP significantly reduced NOX4 protein levels in cells exposed to radiation or cells exposed to the combination of radiation and high glucose (Fig. 2B).

NOX2 is a vital ROS producing NOX enzyme and high glucose alone, radiation alone and the combination of high glucose and radiation significantly increased NOX2 mRNA levels as compared to controls. In fact, NOX2 mRNA levels were increased 15-fold when treated with radiation and high glucose as compared to control groups. MnTE-2-PyP treatment significantly decreased NOX2 mRNA expression in both high glucose or radiated alone conditions (Fig. 2C). However, MnTE-2-PyP treatment did not have any effect on NOX2 mRNA expression in the combination of radiation and high glucose (Fig. 2C).

NOX2 protein expression also did not follow NOX2 mRNA levels. High glucose appeared to have no effect on NOX2 protein levels, while radiation alone or in combination with high glucose significantly reduced NOX2 protein levels (Fig. 2D). The addition of MnTE-2-PyP tended to enhance NOX2 levels back towards control levels in radiated samples in the presence or absence of high glucose; however, these changes were not statistically significant (Fig. 2D).

3. MnTE-2-PyP inhibited NOX2 protein degradation and restored nuclear NOX2 levels after radiation without altering overall nuclear ROS levels

One explanation as to why NOX2 mRNA levels do not follow NOX2 protein levels could be that the NOX2 protein is being degraded rapidly in the irradiated hyperglycemic condition. Therefore, to test this hypothesis, we used the proteasomal inhibitor, MG132, to inhibit protein

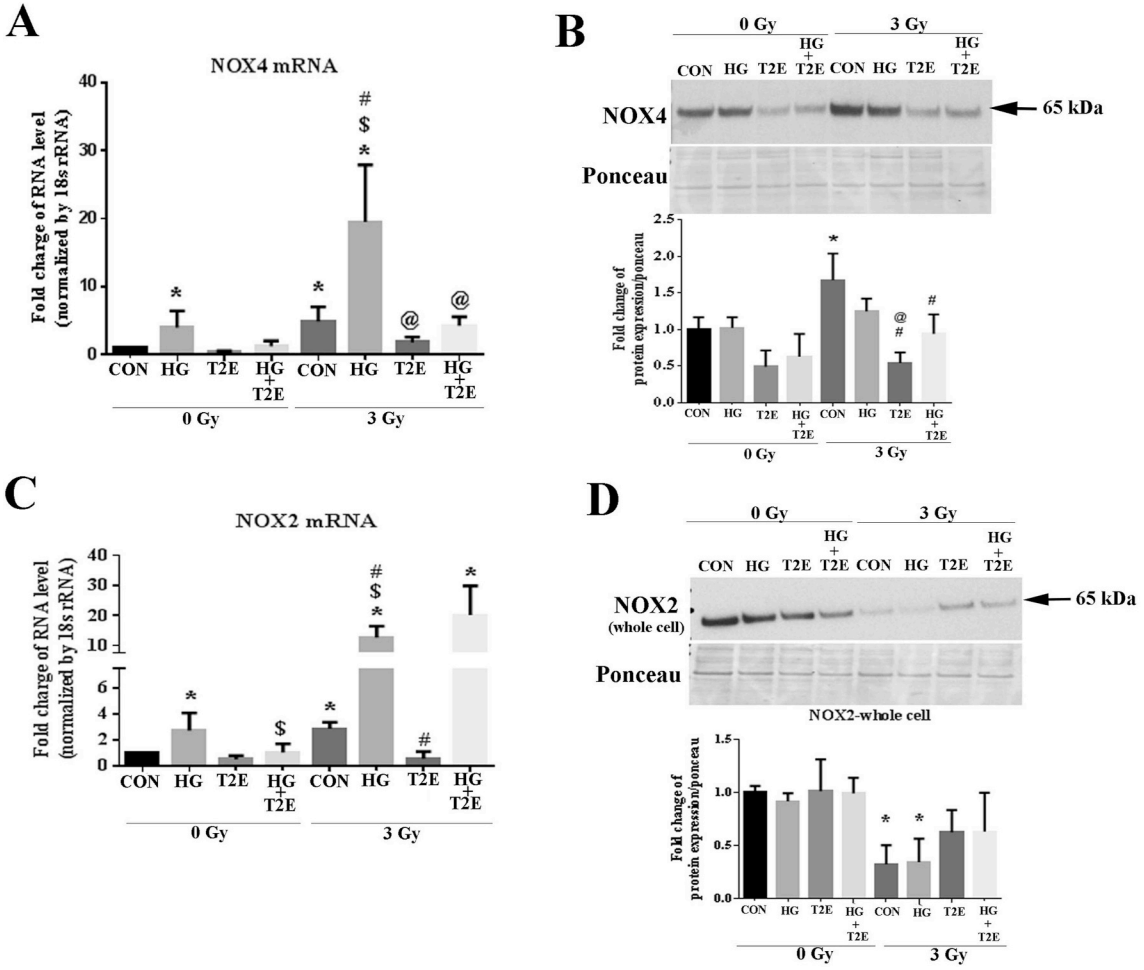


**Fig. 2. MnTE-2-PyP inhibited NOX4 expression and restored NOX2 expression after radiation.** Human prostate fibroblast cells were treated with 20 mM glucose (HG) in the presence or absence of 3 Gy of X-rays (RAD) and 30 μM MnTE-2-PyP (T2E). **A.** NOX4 mRNA expression. NOX4 mRNA was significantly increased in HG alone, radiation alone and RAD + HG group as compared to control. NOX4 mRNA expression was significantly higher in the RAD + HG group as compared to HG and RAD groups. T2E treatment significantly decreased NOX4 mRNA expression after radiation. **B.** NOX4 protein expression. Radiation significantly enhanced NOX4 protein expression. T2E significantly decreased NOX4 protein expression in the irradiated group. **C.** NOX2 mRNA expression. NOX2 mRNA was increased in HG, RAD and RAD + HG groups as compared to control. T2E down regulated NOX2 mRNA expression in HG and RAD groups but not in RAD + HG group. **D.** NOX2 protein expression. NOX2 protein levels were decreased in RAD and RAD + HG group as compared to control. n ≥ 3. (*) denotes a significant difference as compared to control, ($) denotes a significant difference as compared to HG, (#) denotes a significant difference as compared to RAD and (@) denotes a significant difference as compared to RAD + HG group.

degradation through the proteasome pathway. MG132 treatment significantly increased NOX2 levels in the irradiated hyperglycemic condition as compared to control or irradiated hyperglycemic condition alone (Fig. 3A). Thus, we can conclude that NOX2 protein is being degraded, at least in part, through the proteosomal pathway.

Restoration of NOX2 by MnTE-2-PyP in irradiated conditions (Fig. 2D) led us to investigate the effects of MnTE-2-PyP on the subcellular localization of NOX2 in the presence of radiation and high glucose. The combination of radiation and high glucose resulted in a significant decrease in the nuclear localization of NOX2. MnTE-2-PyP treatment significantly increased nuclear localization of NOX2 both in cells exposed to radiation alone and cells exposed to radiation and high glucose (Fig. 3B). We also investigated the effects of radiation and high glucose on NOX2 in the cytoplasmic or mitochondrial fractions and did not observe any significant alteration in cytosolic or mitochondrial NOX2 levels (Supplementary Fig. 1A). The purity of cytosolic, nuclear and mitochondrial protein isolation was verified by GAPDH, Histone1 and TOMM20 western blot by using respective protein fractions (Supplementary Fig. 1B).

Since we have shown that MnTE-2-PyP increases nuclear levels of NOX2, we wanted to determine the effect of MnTE-2-PyP in altering the oxidative state of the nucleus. Overall ROS were measured by dihydroethidium (DHE) staining using confocal microscopy. Using ImageJ software, we quantified ROS staining co-localizing with DAPI (nuclear staining) and found no significant change in nuclear ROS levels in any of the groups tested (Fig. 3C). However, overall cellular ROS was significantly enhanced in the radiation, high glucose, and combination of radiation and high glucose and MnTE-2-PyP treatment abolished these increases (Fig. 1C). This indicates that MnTE-2-PyP is scavenging overall ROS but maintaining basal ROS levels in the nucleus.

4. MnTE-2-PyP decreased DNA binding of p50 subunit of NF-κB through NOX2-mediated oxidation of nuclear thioredoxin (Trx)

We showed that NOX4 is downregulated by MnTE-2-PyP treatment (Fig. 2). A known transcriptional regulator of NOX4 is NF-κB, which induces inflammation. MnTE-2-PyP mediated protection from inflammation was reported before [23,35]. Therefore, we investigated the effects of radiation, high glucose and MnTE-2-PyP on NF-κB expression and activity via DNA binding. The nuclear levels of p65 subunits of NF-κB were significantly lower in radiation and the combination of radiation and high glucose as compared to control. MnTE-2-PyP treatment

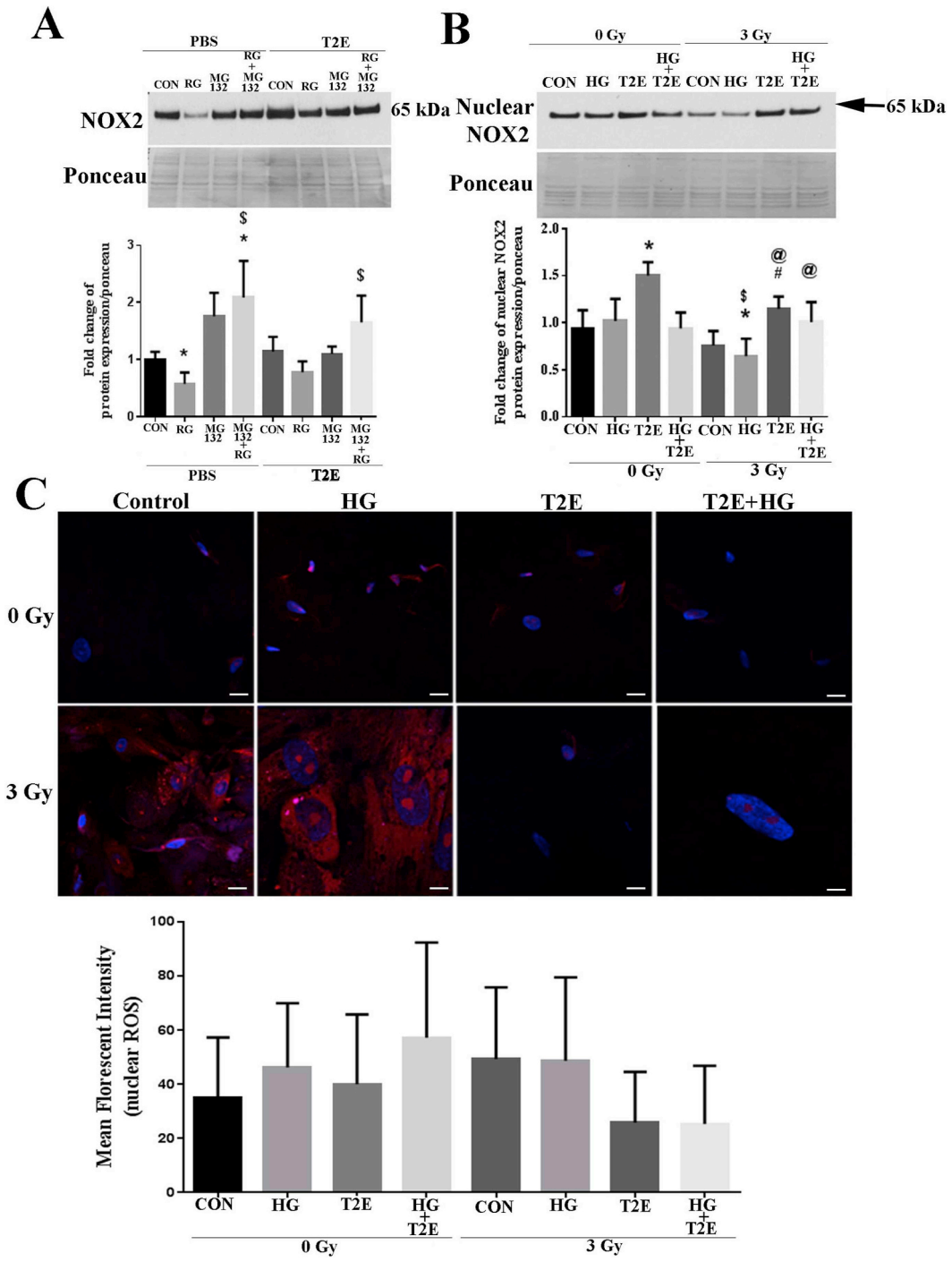


**Fig. 3. MnTE-2-PyP inhibited NOX2 protein degradation and restored nuclear NOX2 levels after radiation without altering overall nuclear ROS levels. A.** NOX2 protein stability. Human prostate fibroblast cells were treated with 20 mM glucose and 3 Gy of X-rays (RG) in the presence or absence of 30 μM MnTE-2-PyP (T2E) and 0.5 μM MG132 (added 30 min before radiation). NOX2 levels was significantly lower in the RG group as compared to control. MG132 significantly increased NOX2 levels. T2E treatment increased NOX2 levels in MG132 treated samples exposed to RG condition. n ≥ 3. (*) denotes a significant difference as compared to control and ($) denotes a significant difference as compared to RG group. **B.** NOX2 nuclear protein expression. Human prostate fibroblast cells were treated with 20 mM glucose (HG) in the presence or absence of 3 Gy of X-rays (RAD) and 30 μM MnTE-2-PyP (T2E). Nuclear NOX2 levels were significantly reduced in RAD + HG group as compared to control and HG only. T2E treatment enhanced nuclear NOX2 levels in the radiated conditions. n ≥ 3. (*) denotes a significant difference as compared to control, ($) denotes a significant difference as compared to HG, (#) denotes a significant difference as compared to RAD and (@) denotes a significant difference as compared to RAD + HG group. **C.** Cells were stained with DHE (red) and DAPI (blue). n ≥ 3. Images were analyzed by measuring DHE mean florescent intensity in the nucleus. The scale bar = 20 μm. No significant changes were observed. (For interpretation of the references to colour in this figure legend, the reader is referred to the Web version of this article.)

restored the p65 levels to the control in these two irradiated groups (Fig. 4A). In contrast, nuclear levels of the p50 were significantly higher in irradiated hyperglycemic group as compared to control, high glucose alone, and radiation alone treatments. MnTE-2-PyP treatment significantly decreased nuclear p50 levels in the radiation and high glucose treated group (Fig. 4A).

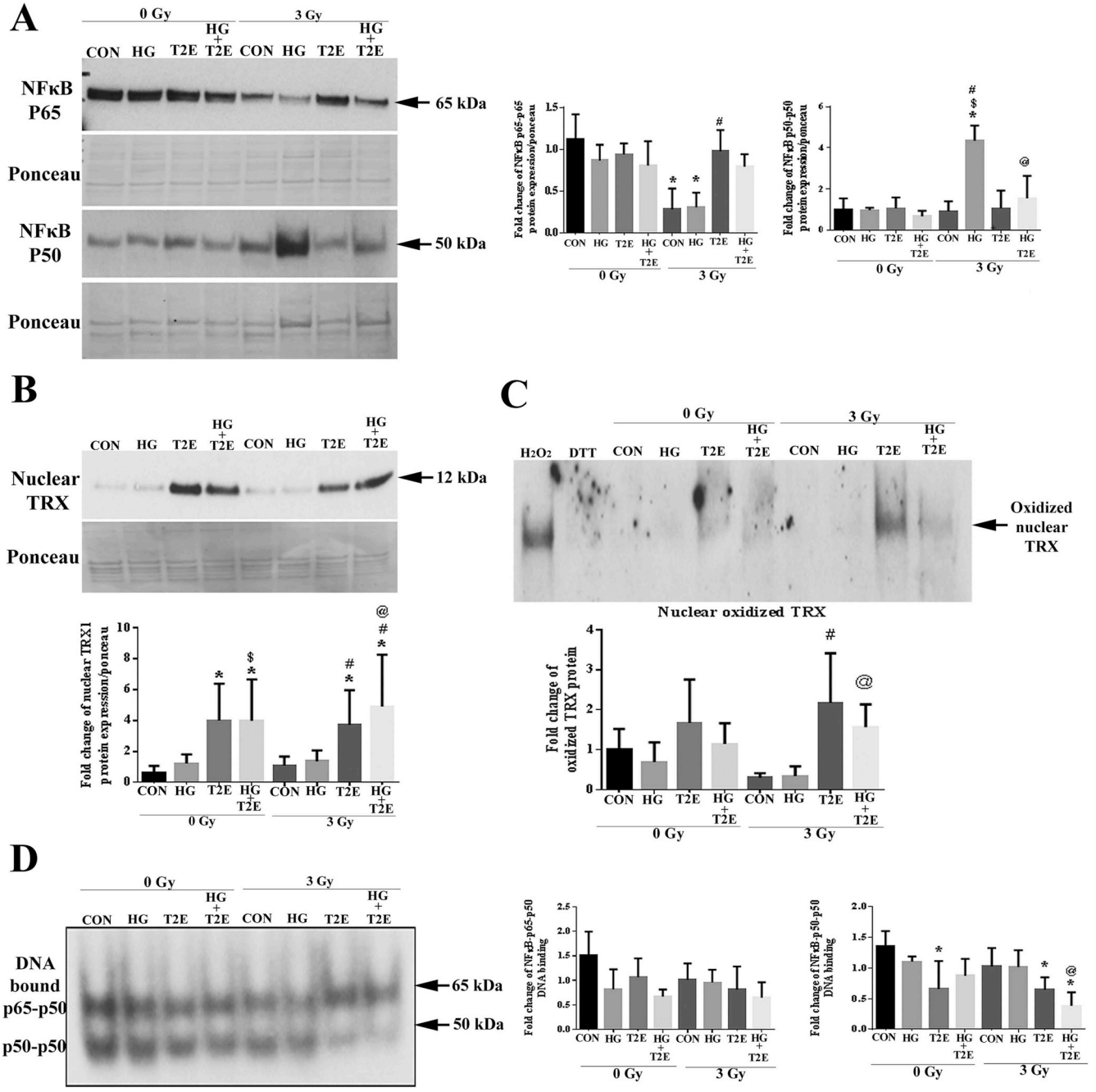


**Fig. 4. MnTE-2-PyP decreased DNA binding of p50 subunit of NF-κB through NOX2 mediated oxidation of nuclear Trx.** Human prostate fibroblast cells were treated with 20 mM glucose (HG) in the presence or absence of 3 Gy of X-rays (RAD) and 30 μM MnTE-2-PyP (T2E). **A.** Nuclear NFκB levels. NFκB p65 levels were significantly lower in RAD and RAD + HG groups as compared to control. T2E treatment restored NFκB p65 levels. NFκB p50 levels were significantly higher in RAD + HG group, which were suppressed by T2E. **B.** Nuclear thioredoxin (TRX) protein expression. T2E treatment significantly increased nuclear TRX levels in radiated and non-radiated conditions. **C.** Oxidized nuclear TRX protein levels. T2E treatment significantly increased oxidized nuclear TRX levels. The fully oxidized upper band of TRX is represented on a redox western blot. **D.** NFκB EMSA. DNA binding of NFκB p65-p50 heterodimer and p50-p50 homodimer. p65-p50 DNA binding was not altered. The DNA binding of p50-p50 homodimer was significantly less in T2E treatment after radiation. n ≥ 3. (*) denotes a significant difference as compared to control, ($) denotes a significant difference as compared to HG, (#) denotes a significant difference as compared to RAD and (@) denotes a significant difference as compared to RAD + HG group.

However, nuclear localization does not necessarily correlate to NF-κB activity. It is reported that nuclear accumulation of NOX2 oxidizes nuclear Trx. Oxidized Trx can no longer reduce p50, and the Cys62 of the p50 subunit of NF-κB must be in its reduced form for maintaining optimum DNA binding [36,37]. Therefore, nuclear NOX2 oxidizes Trx, which inhibits DNA binding of p50. It was found that nuclear Trx levels were very low in control or cells exposed to high glucose alone, radiation alone or the combination of radiation and high glucose (Fig. 4B). However, MnTE-2-PyP increased nuclear Trx levels in every condition tested (Fig. 4B).

The redox status of Trx was then investigated. Nuclear protein extracts from $H_2O_2$ and DTT treated cells were used as oxidized and reduced controls respectively. Levels of fully oxidized nuclear Trx were significantly increased in MnTE-2-PyP treated cells both in normoglycemic and hyperglycemic irradiated conditions as compared to radiation alone and radiation and high glucose treated conditions

(Fig. 4C). Whereas total levels of Trx in the cytosol were not altered significantly (Supplementary Fig. 2).

It has been reported previously that MnTE-2-PyP alters NF-κB DNA binding by oxidizing the p50 subunit of NF-κB [26,38]. Our data also demonstrates an accumulation of NOX2 and oxidized Trx in the nucleus in the irradiated conditions after MnTE-2-PyP treatment. All these data indicate that MnTE-2-PyP likely reduces the DNA binding activity of NF-κB. First, we investigated the DNA binding activity of NF-κB by EMSA and found no significant difference in the ability of the p65-p50 heterodimer to bind to DNA in any of the conditions (Fig. 4D). However, as expected, the DNA binding of p50-p50 homodimer was significantly lower in irradiated conditions when MnTE-2-PyP is added as compared to the control (Fig. 4D). Thus, in MnTE-2-PyP treated irradiated conditions, nuclear accumulation of NOX2 increases the oxidation of nuclear Trx, which results in the oxidation and loss of optimal DNA binding of the p50-p50 homodimer of NF-κB.

## 5. MnTE-2-PyP enhanced NRF2 levels

NRF2 is a transcription factor that is a master regulator of the antioxidant defense system and is often upregulated during cellular stress. We have recently shown that levels of NQO1, a NRF2 target protein, is elevated in fibroblast cells after treatment with MnTE-2-PyP [23]. Therefore, we investigated NRF2 levels in the context of high glucose and radiation. We observed that NRF2 levels were significantly lower in irradiated cells and cells irradiated in the presence of high glucose as compared to control cells (Fig. 5A). NRF2 levels are also significantly lower in the radiation and high glucose group as compared to the high glucose alone group. In agreement with previous findings, MnTE-2-PyP significantly increased NRF2 levels as compared to control, high glucose and radiation alone treatments (Fig. 5A). To further confirm these results, immunostaining for NRF2 was performed and the combination of radiation and high glucose resulted in a reduction in overall NRF2 staining, which was reversed by the addition of MnTE-2-PyP. In the presence of radiation, MnTE-2-PyP treatment also significantly increased NRF2 nuclear localization (Fig. 5B).

To activate antioxidant signaling, NRF2 needs to localize to the nucleus to induce antioxidant response element (ARE) mediated antioxidant gene expression. Therefore, we investigated the subcellular localization of NRF2. Cytosolic NRF2 levels were significantly reduced in the combination of radiation and high glucose as compared to high glucose alone groups. MnTE-2-PyP treatment significantly increased cytosolic NRF2 levels in all conditions regardless of radiation or high glucose levels (Fig. 5C). Nuclear NRF2 levels were also significantly lower in radiation alone or radiation and high glucose groups as compared to the control (Fig. 5D). MnTE-2-PyP treatment significantly enhanced NRF2 nuclear levels in every condition as compared to their respective controls, indicating that the level of NRF2 is increased both in the cytosol and nucleus with MnTE-2-PyP treatment.

## 6. MnTE-2-PyP enhanced NRF2 and AP-1-mediated transcriptional activity

As nuclear localization of NRF2 was increased by MnTE-2-PyP treatment, we investigated the DNA binding activity of NRF2. Radiation and/or high glucose did not affect NRF2 DNA binding. In normal glycemic conditions, MnTE-2-PyP, alone or in combination with radiation, significantly increased NRF2 DNA binding when compared to controls (Fig. 6A). Surprisingly, MnTE-2-PyP was unable to enhance NRF2 DNA binding in high glucose treated cells both in irradiated and non-irradiated conditions. Thus, even though NRF2 levels were enhanced in the cells treated with high glucose and radiation, the NRF2 was not able to bind to the DNA in hyperglycemic conditions.

Antioxidant defense can also be achieved through the NRF2/activator protein-1 (AP-1) composite pathway, which does not need NRF2 to bind to DNA directly. The availability of NRF2 in the nucleus, along with Trx and AP-1, results in AP-1 mediated activation of secondary antioxidant signaling pathways [39,40]. AP-2 has also been shown to be involved in NRF2-mediated antioxidant signaling in a promoter specific way. Therefore, we investigated the DNA binding activity of AP-1 and AP-2 in our study. No significant differences in AP-2 DNA binding were observed in any of the conditions tested (data not shown). However, in hyperglycemic conditions, MnTE-2-PyP significantly increased AP-1 DNA binding as compared to control samples (Fig. 6B). Therefore, we can conclude that, both in irradiated and non-irradiated conditions MnTE-2-PyP increases DNA binding of NRF2 when the glycemic level is normal, which directly increases NRF2 mediated antioxidant signaling. While, in a hyperglycemic environment, MnTE-2-PyP increases AP-1 DNA binding and increases the nuclear localization of NRF2 and Trx. We hypothesize that in hyperglycemia, MnTE-2-PyP increases the NRF2/AP-1 composite pathway to increase antioxidant signaling. Therefore, both in normal and hyperglycemia, MnTE-2-PyP treatment will induce antioxidant signaling. To study this hypothesis, we have measured NQO1 protein levels. NQO1 is a direct downstream target for NRF2 and is also a target for the NRF2/AP-1 composite pathway. As expected, NQO1 levels were significantly lower in radiation alone and radiation and high glucose groups as compared to controls. MnTE-2-PyP significantly increased NQO1 levels in all conditions as compared to control (Fig. 6C). Our investigation demonstrated that in hyperglycemia, antioxidant signaling is activated, via NQO1 expression, not by direct DNA binding of NRF2 but likely by the combined action of NRF2, Trx and AP-1.

We next wanted to determine how vital the role of NRF2 is in MnTE-2-PyP mediated anti-fibrotic action in an irradiated hyperglycemic environment. NRF2 was knocked down (Fig. 6D) by siRNA and cells were exposed to radiation and hyperglycemia in the presence or absence of MnTE-2-PyP. In the control siRNA group, radiation and high glucose resulted in an expected upregulation of α-SMA expression and MnTE-2-PyP significantly downregulated α-SMA expression both in control and combined radiation and high glucose conditions. In cells treated with NRF2 siRNA, there was a significant upregulation of α-SMA expression in all the conditions as compared to cells treated with control siRNA (Fig. 6D). NRF2 knockdown increases α-SMA expression in all the conditions and this result suggests that NRF2 is a vital regulator for α-SMA. MnTE-2-PyP was unable to reduce α-SMA levels back to control levels when NRF2 was reduced. However, we noticed that after NRF2 knockdown, MnTE-2-PyP decreased α-SMA expression in radiation and high glucose treated cells as compared to PBS, radiation and high glucose treated NRF2 knocked down cells (Fig. 6D). This observation opens a possibility that MnTE-2-PyP is not solely dependent on NRF2, to reduce fibrotic signaling.

## 7. In combination with high glucose and radiation, MnTE-2-PyP treated prostate fibroblast cells enhanced prostate cancer cell death

In an *in vivo* environment, the stromal layer surrounds the prostate glandular regions in a normal prostate. The stromal fibroblast layer infiltrates in between the glandular region as the prostate tumor progresses [41]. During diabetic tumor progression, the stromal fibroblast cells will be in close proximity to the cancerous epithelial cells. Therefore, to investigate the role of prostate fibroblasts on the cancer cells, we treated PC-3 (a representative of late neuroendocrine type prostate cancer) and LNCaP (a representative of early state androgen sensitive prostate cancer) cells with conditioned media from prostate fibroblast cells treated either with high glucose alone, radiation alone, or the combination of high glucose and radiation in the presence or absence of MnTE-2-PyP. Cancer cell viability was measured four days after incubation with the conditioned media from the fibroblast cells.

PC-3 cell death was significantly increased, 3–4 fold, when treated with the conditioned media collected from MnTE-2-PyP treated irradiated human prostate fibroblast cells or conditioned media from MnTE-2-PyP, high glucose and radiation treated fibroblast cells

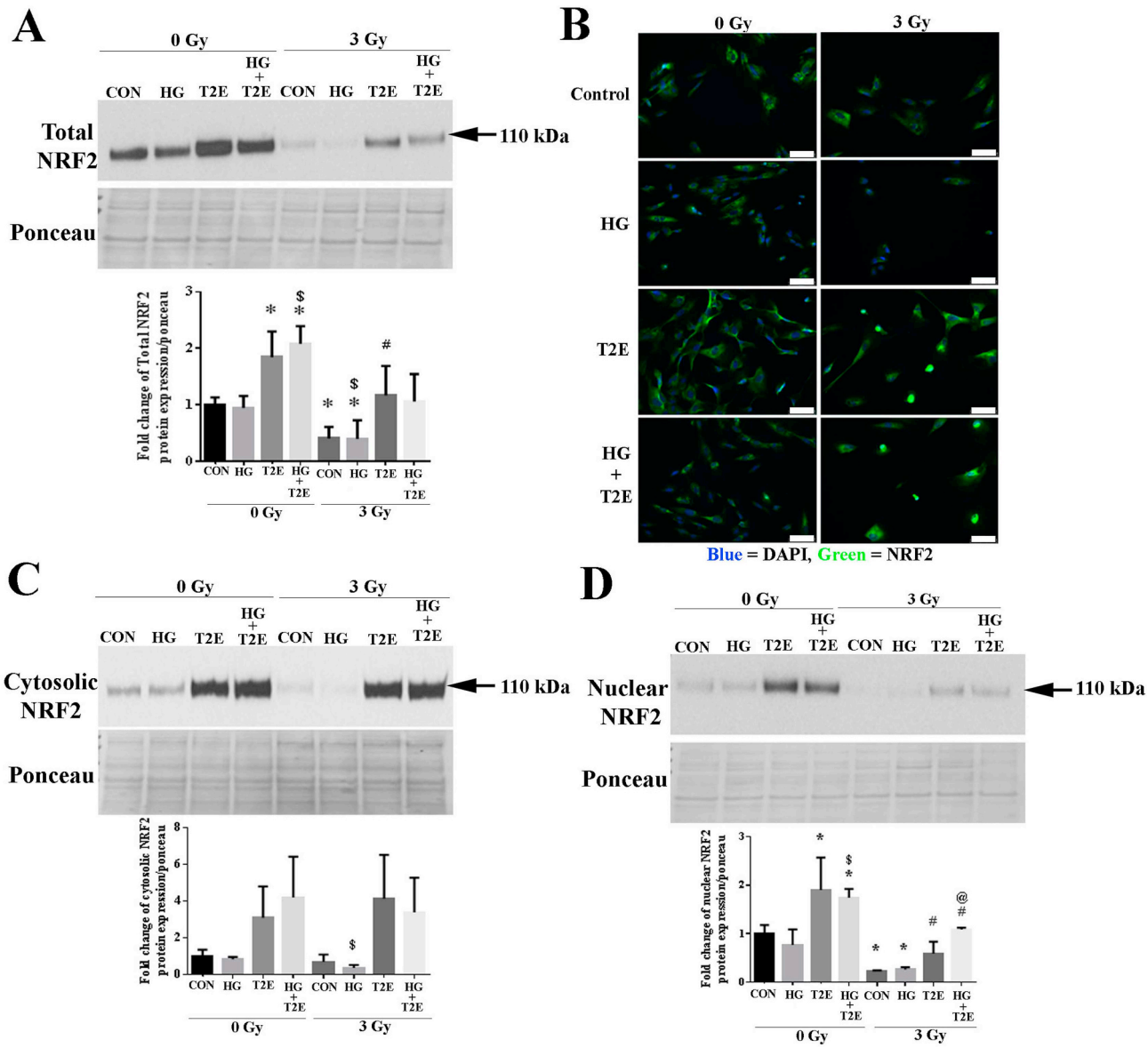


**Fig. 5. MnTE-2-PyP enhanced NRF2 levels.** Human prostate fibroblast cells were treated with 20 mM glucose (HG) in the presence or absence of 3 Gy of X-rays (RAD) and 30 μM MnTE-2-PyP (T2E). **A.** Total NRF2 protein expression. T2E increased total NRF2 protein levels in whole cell extracts in irradiated and non-irradiated conditions. **B.** NRF2 protein visualized by immunofluorescence. Immunofluorescence staining showed a decrease in NRF2 (green fluorescence) in irradiated and HG treated cells and T2E enhanced NRF2 expression. In irradiated cells, T2E treatment enhanced nuclear (blue) localization of NRF2. The scale bar = 100 μm. **C.** Cytosolic NRF2 protein expression. Cytosolic NRF2 levels were significantly lower in the RAD + HG group as compared to the HG group and T2E treatment increased cytosolic NRF2 levels. **D.** Nuclear NRF2 protein expression. Nuclear NRF2 levels were significantly lower in radiated conditions as compared to control. T2E treatment significantly upregulated nuclear NRF2 levels in control, HG, RAD and RAD + HG conditions. n ≥ 3. (*) denotes a significant difference as compared to control, ($) denotes a significant difference as compared to HG, (#) denotes a significant difference as compared to RAD and (@) denotes a significant difference as compared to RAD + HG group. (For interpretation of the references to colour in this figure legend, the reader is referred to the Web version of this article.)

(Fig. 7A). Cell death of LNCaP cells was also significantly increased when treated with conditioned media. Specifically, conditioned media from MnTE-2-PyP treated fibroblast cells that were exposed to high glucose alone or high glucose in combination with radiation resulted in a significant increase in cell death (2–3 fold increases in cell death). Interestingly, in LNCaP cells, combination of high glucose and radiation resulted in about a 2 fold increase in cell death (Fig. 7B). However, in PC-3 cells, the combination of high glucose and radiation had no effect on cell death (Fig. 7A). Treatment of conditioned media from MnTE-2-PyP treated fibroblasts (which are protected from radiation and hyperglycemia-induced damage) enhanced prostate cancer cell death.

To determine the direct effect that hyperglycemia, radiation and MnTE-2-PyP have on PC-3 and LNCaP cell viability, the cancer cells were treated directly with these conditions. We found that radiation combined with hyperglycemia caused a significant increase in LNCaP cell death (Fig. 7D), which is a radiosensitive cell line. PC-3 cell viability was not significantly altered with any direct treatment. MnTE-2-PyP did not show any significant effect directly on PC-3 or LNCaP cells in any of the conditions tested (Fig. 7C and D). Therefore, the increased cell death observed with conditioned media from MnTE-2-PyP and radiation treated fibroblasts, is due to the effect of the fibroblasts and not due to the effect of MnTE-2-PyP and radiation directly on the cancer cells.

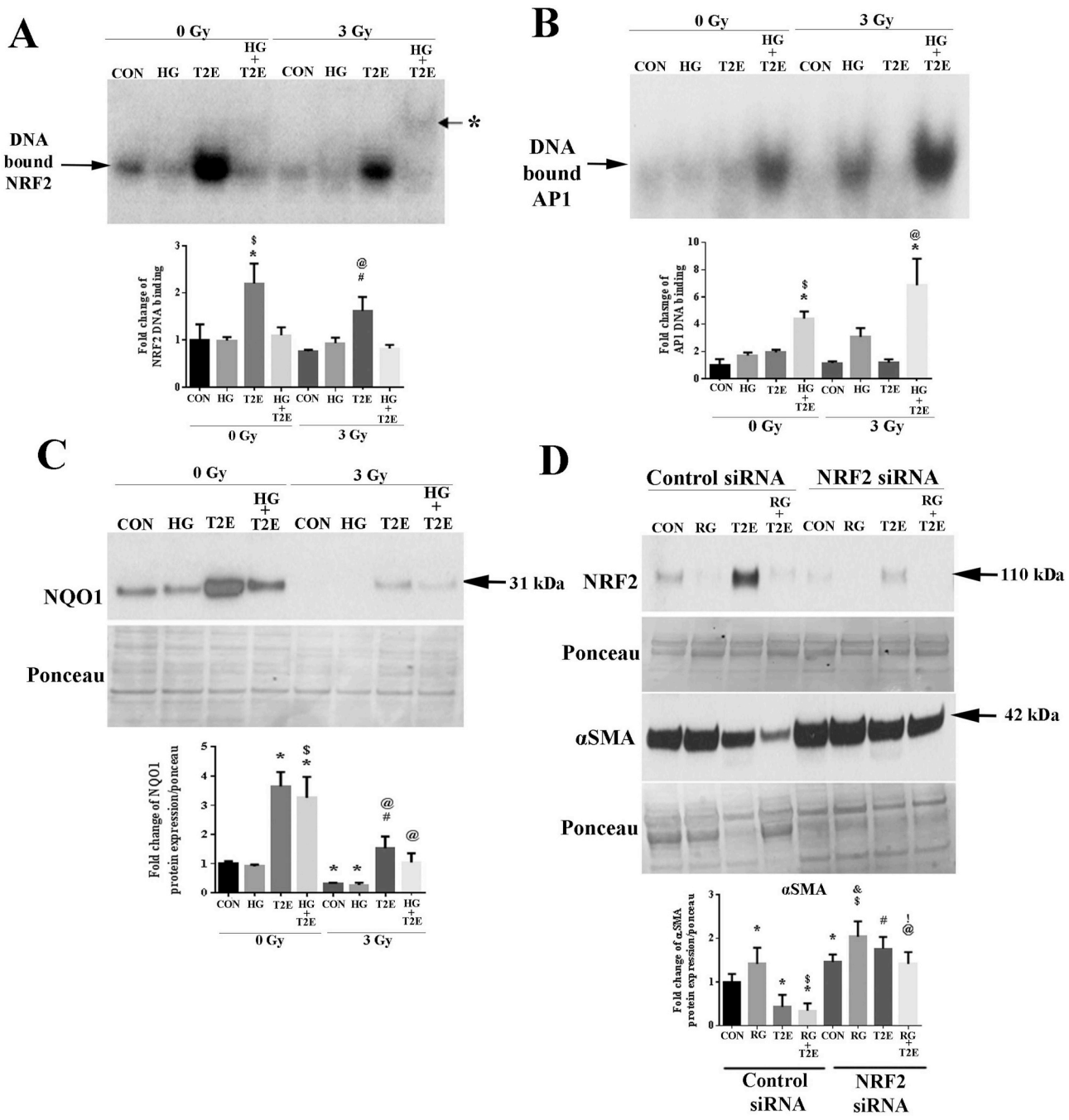


**Fig. 6. MnTE-2-PyP enhanced NRF2 and AP1-mediated transcriptional activity.** Human prostate fibroblast cells were treated with 20 mM glucose (HG) in the presence or absence of 3 Gy of X-rays (RAD) and 30 μM MnTE-2-PyP (T2E). **A.** NRF2 EMSA. DNA binding of NRF2 was significantly increased by T2E treatment in irradiated and non-irradiated normo-glycemic conditions [asterisk (*) indicates a weak signal for DNA binding at a higher position in RAD + HG + T2E treatment]. **B.** AP1 EMSA. DNA binding of AP1 was significantly increased by T2E treatment in irradiated and non-radiated hyperglycemic conditions. **C.** NQO1 protein expression. Both in hyperglycemia and normoglycemia, T2E increased NQO1 expression irrespective of radiation treatment. **D.** Human prostate fibroblast cells were either transfected with control siRNA or NRF2 siRNA followed by treatment with 20 mM glucose and 3 Gy of X rays (RG) in the presence or absence of 30 μM MnTE-2-PyP (T2E). NRF2 was successfully knocked down in NRF2 siRNA treated cells. NRF2 knock down by siRNA treatment increased α-SMA expression in control and RAD + HG (RG) treatment. T2E mediated suppression of α-SMA was inhibited by NRF2 knock down. In RG condition, T2E was able to downregulate α-SMA expression even in the absence of NRF2 (lane 8 compared to lane 6). n ≥ 3. For A, B and C: (*) denotes a significant difference as compared to control, ($) denotes a significant difference as compared to HG, (#) denotes a significant difference as compared to RAD and (@) denotes a significant difference as compared to RAD + HG group. For D: (*) denotes a significant difference as compared to control siRNA-control, ($) denotes a significant difference as compared to control siRNA -RG, (#) denotes a significant difference as compared to control siRNA-T2E, (@) denotes a significant difference as compared to control siRNA-T2E + RG, (&) denotes a significant difference as compared to NRF2siRNA-control and (!) denotes a significant difference as compared to NRF2siRNA-RG.

## 4. Discussion

It is well established that diabetics suffer from cellular damage caused by glucose induced stress and ROS [42,43], which results in enhanced radiation damage [8–10]. In our *in vitro* model, we demonstrated that using 20 mM glucose and 3 Gy of X-rays, mimics a diabetic irradiated condition. Specifically, we found that radiation and high glucose caused more fibroblast cell death, increased cellular ROS levels,

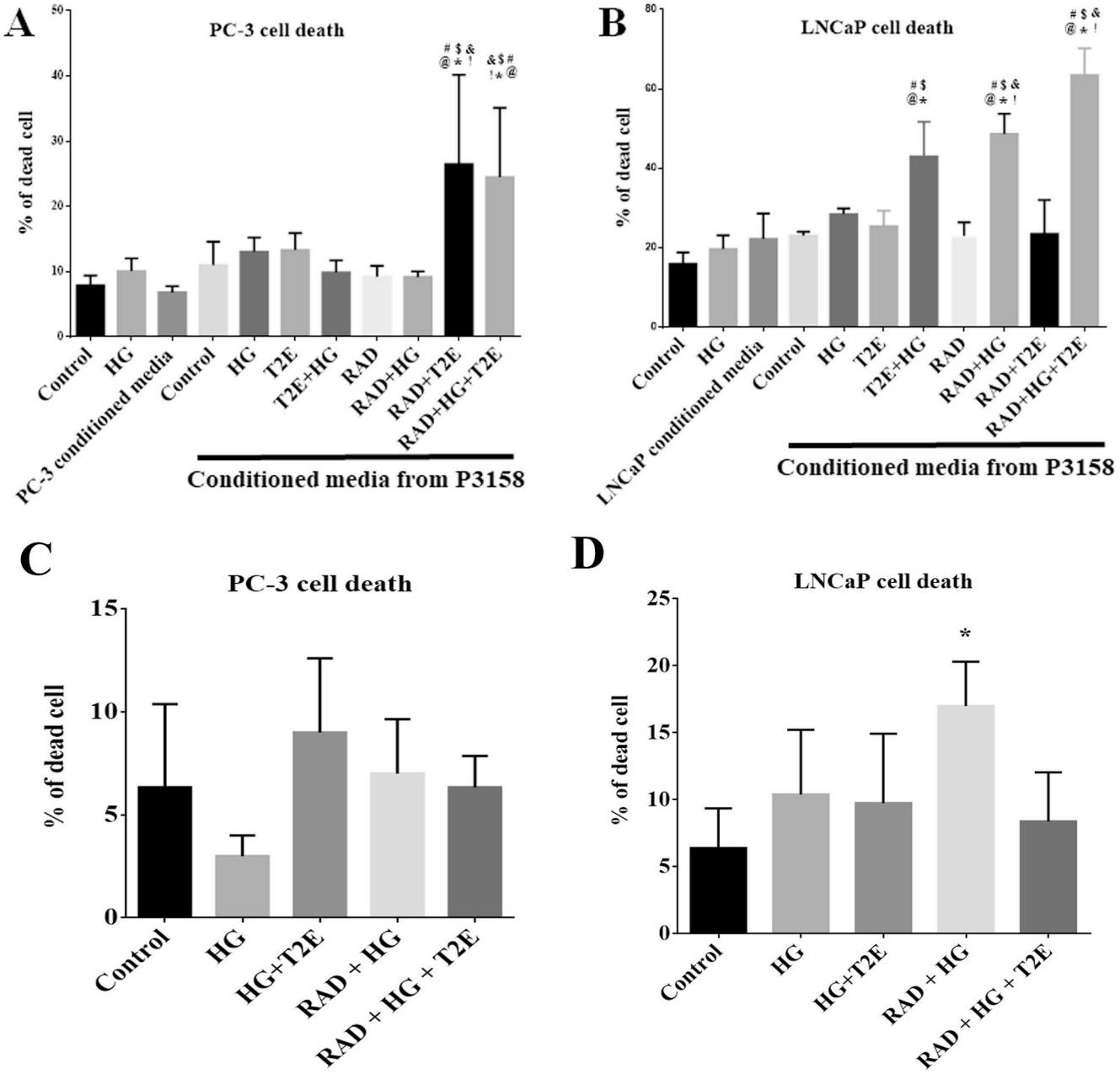


**Fig. 7. Under high glucose and radiation, MnTE-2-PyP treated prostate fibroblast cells enhanced prostate cancer cell death.** Human prostate cancer cells, PC-3 and LNCaP were treated with only PBS (Control), 20 mM glucose (HG), PC-3 or LNCaP conditioned media or different combinations of conditioned media (CM) collected from human prostate fibroblast cells (P3158). **A.** PC-3 cell death. CM-P3158-RAD + T2E and CM-P3158-RAD + HG + T2E significantly increased PC-3 cell death. **B.** LNCaP cell death. CM-P3138-T2E + HG, CM-P3158-RAD + HG and CM-P3158-RAD + HG + T2E significantly increased LNCaP cell death. PC-3 and LNCaP cells treated directly with 20 mM glucose (HG), 3 Gy X-radiation (RAD) or both in presence or absence of 30 μM MnTE-2-PyP (T2E). **C.** PC-3 cell death. No significant change in percentage of cell death was noticed in any of the conditions. **D.** LNCaP cell death. RAD + HG treatment significantly increased LNCaP cell death compared to control. n = 3. (*) denotes a significant difference compared to control.

For Fig. 7A: n = 4. (*) denotes a significant difference as compared to Control, ($) denotes a significant difference as compared to HG, (#) denotes a significant difference as compared to CM-PC3, (@) denotes a significant difference as compared to CM-P3158-Control, (&) denotes a significant difference as compared to CM-P3158-RAD and (!) denotes a significant difference as compared to the CM-P3158-RAD + HG group.

For Fig. 7B: n = 3. (*) denotes a significant difference as compared to Control, ($) denotes a significant difference as compared to HG, (#) denotes a significant difference as compared to the CM-LNCaP, (@) denotes a significant difference as compared to CM-P3158-Control, (&) denotes a significant difference as compared to CM-P3158-HG and (!) denotes a significant difference as compared to CM-P3158-RAD group.

and enhanced pro-fibrotic signaling. The addition of MnTE-2-PyP protected from cell death, reduced cellular ROS and inhibited fibrotic signaling during hyperglycemia and/or radiation. Thus, the data indicates that not only in radiation-mediated fibrosis, MnTE-2-PyP can be a strong therapeutic candidate to combat diabetes-mediated tissue fibrosis irrespective of radiation. This expands the therapeutic ability of MnTE-2-PyP beyond its activity as a radioprotector.

NOX enzymes and mitochondrial-mediated ROS increase AGE-RAGE signaling in a diabetic environment, which creates a feed forward loop to produce more ROS in the system [44–46]. Elevated ROS in diabetics promotes inflammation and tissue damage over time. Upregulation of the pro-inflammatory NF-κB pathway under oxidative stress

is, in part, a causal agent for inflammation and fibrosis via TGF-β signaling. Thus, the systemic environment of a diabetic is inflamed, oxidatively stressed, and prone to fibrosis [16–19,28]. NOX enzymes drive damage both in diabetics as well in irradiated normal tissues. Therefore, we studied the role of various NOX proteins, specifically NOX1, NOX4 and NOX2 expression levels in this study. We did not find any significant difference in NOX1 protein levels; however, NOX4 and NOX2 protein levels were significantly altered. Specifically, the radiation and high glucose condition resulted in a 1.5 fold increase in NOX4 protein expression. In contrast, MnTE-2-PyP reduced NOX4 protein expression both in irradiated and non-irradiated conditions irrespective of glycemic conditions (Fig. 2B). NOX4 is one of the major sources of ROS during radiation and has been shown to upregulate α-SMA. Accordingly, α-SMA expression followed NOX4 expression and MnTE-2-PyP inhibited both of these proteins.

NOX2 protein expression was the direct opposite of NOX4 expression. A significant downregulation of NOX2 protein expression was observed in radiation and radiation + high glucose group as compared to control. MnTE-2-PyP treatment increased NOX2 protein expression in radiated conditions back to control levels. We hypothesized that NOX2 protein was degraded, which was inhibited by MnTE-2-PyP to maintain the NOX2 protein levels similar to control levels. To investigate this idea, we inhibited the proteasomal protein degradation pathway by MG132. As expected, MG132 treatment protected radiation + high glucose mediated degradation of NOX2 protein.

It is reported that, NOX2 protects against prolonged inflammation [47]. To delineate the cytoprotective action of NOX2 in MnTE-2-PyP treated cells after radiation, we investigated the subcellular localization of NOX2 protein. Our study revealed that in the radiated conditions, only nuclear NOX2 protein levels were decreased, which was significantly restored to control levels by MnTE-2-PyP treatment. To maintain normal physiological activity, nuclear ROS needs to be maintained optimally in cells [48]. Nuclear NOX2 restoration by MnTE-2-PyP did not alter nuclear ROS levels. It has been reported that NOX2 deficiency leads to hyper-inflammation in the case of antimicrobial host defense [49]. One of the major inflammatory molecules regulated by NOX2 is NF-κB, which is a vital regulator of cell survival. It is reported that for efficient and effective DNA binding, the cysteine 62 of the NF-κB p50 subunit must be in a reduced form [50,51]. The redox state of cysteine 62 of the NF-κB p50 subunit is regulated by Trx1 [36]. In a pro-inflammatory environment, the presence of Trx1 in the nucleus, the cysteine 62 of the NF-κB p50 subunit will become reduced and allow for efficient DNA binding. It has been reported that NOX2 regulates NF-κB DNA binding by modifying the redox state of Trx1 [37]. The p40phox subunit of NOX2 binds and oxidizes Trx1 to inactivate it. Therefore, in the presence of NOX2 in the nucleus, oxidized Trx1 is unable to reduce the p50 subunit of NF-κB. Thus, NOX2 deficiency causes reductive stress in the cells, which causes an accumulation of reduced Trx1 in the nucleus, which in turn enhances transcriptional activity of NF-κB [37].

Our data showed that, in irradiated conditions, MnTE-2-PyP treatment increased nuclear levels of NOX2 and Trx and increased the oxidation of nuclear Trx. Thus, leading to inefficient DNA binding of p50. Increased oxidation of Trx also explains why the nuclear ROS levels were not altered significantly despite nuclear accumulation of NOX2 in the radiated MnTE-2-PyP treated conditions. However, it is necessary to investigate the redox state of Trx in the nucleus in presence of MnTE-2-PyP in a NOX2 inhibited condition. Our study also revealed that the DNA binding of p50 was significantly reduced in MnTE-2-PyP treatment after radiation, but the DNA binding of p65 was not altered significantly. Therefore, after radiation, irrespective of glycemic condition, MnTE-2-PyP suppresses p50 DNA binding specifically. MnTE-2-PyP mediated inhibition of NF-κB p50 DNA binding has previously been reported in a diabetic environment, where p65-p50 activity were unaltered [27,28,52]. Batinic-Haberle et al. proposed a pro-oxidative effect of MnTE-2-PyP in the nucleus that results in reduced p50 DNA binding [24].

We have previously shown that, MnTE-2-PyP enhances the expression of NQO1 [23], a detoxifier of quinones [53]. This study revealed that, MnTE-2-PyP treatment also enhances the protein expression levels of another cytoprotective antioxidant enzyme, Trx. Both NQO1 and Trx are downstream targets of the NRF2-ARE antioxidant pathway [54]. NRF2 is one of the major transcriptional regulators of cytoprotective antioxidant enzymes such as, NQO1, Trx, HO-1, SOD1, catalase and GPx, against oxidative stress. During an oxidative insult, NRF2 dissociates from KEAP1 avoiding degradation in the cytosol and translocates to the nucleus to activate its transcriptional activity to detoxify superoxide and hydrogen peroxide [55–58]. Under excessive oxidative stress and an impaired antioxidant defense system such as in diabetics, NRF2-mediated antioxidant defense is not activated resulting in oxidative damage to macromolecules [56,58]. In high fat diet induced diabetes, NRF2 maintains self-repair and function of the pancreatic β cells [55]. Therefore, activation of NRF2 is considered an important therapeutic target for controlling diabetes mediated oxidative stress [56]. We have recently shown that in a normo-glycemic environment, MnTE-2-PyP increases NRF2 activity [59]. In mouse hematopoietic stem/progenitor cells, a similar manganese porphyrin, MnTnBuOE-2-PyP increased NRF2 activity [60]. Our study revealed, both in normoglycemic and hyperglycemic conditions, total NRF2 protein levels were significantly downregulated by radiation and MnTE-2-PyP enhanced nuclear as well as cytosolic NRF2 levels irrespective of irradiation and hyperglycemia. We further found that MnTE-2-PyP significantly increased DNA binding of NRF2 in irradiated and non-irradiated conditions in a normo-glycemic environment. To our surprise, in a hyperglycemic environment, MnTE-2-PyP was unable to increase NRF2 DNA binding. It is reported that NRF2 can be acetylated by p300, which enhances its DNA binding and transcriptional activity [61]. Other proteins like nucleosome remodelers, chromatin remodeling proteins and sirtuins can physically interact with NRF2 to transcribe the antioxidant enzymes including NQO1 and Trx1 [62–64].

Our further investigation revealed that, MnTE-2-PyP significantly increased DNA binding of AP-1 exclusively in hyperglycemic conditions. Interestingly, AP-2 DNA binding was not altered in MnTE-2-PyP treatment. The NRF2 binding site, ARE, often overlaps with the AP-1 binding site, 12-O-tetradecanoylphorbol-13-acetate response element (TRE) [65,66]. Therefore NRF2/AP-1 functions as a composite circuit. Nuclear Trx is another positive component in this circuit [67–69]. Both AP-1 and AP-2 binding sites are present in the NQO1 promoter [70,71]. AP-1 is considered as a secondary antioxidant response factor [72]. AP-1 can act as a backup for NRF2 activity and play an equal role in antioxidant defense [73]. Therefore, from our study we can conclude that, in a normo-glycemic state, MnTE-2-PyP restores the classical NRF2 mediated antioxidant response. In hyperglycemic conditions, MnTE-2-PyP activates the NRF2/AP-1 composite secondary antioxidant response, in the presence of nuclear NRF2 and Trx. As a result, both in normo-glycemic and hyperglycemic conditions, MnTE-2-PyP can activate NQO1 expression.

To determine the role of NRF2 in the protection of the fibroblast activation in the irradiated diabetic state, NRF2 was knocked down by siRNA. NRF2 knockdown resulted in a significant increase in α-SMA, which indicates a vital role of NRF2 in profibrotic signaling. However, in a NRF2 knocked down condition, radiation + high glucose mediated increase in α-SMA level was suppressed to some extent by MnTE-2-PyP treatment. This indicates that MnTE-2-PyP may inhibit fibrotic signaling through NRF2 dependent and independent pathways. Some NRF2 independent pathways may be the direct scavenging of superoxide by MnTE-2-PyP or the inhibition of the NOX4/TGFβ1 pathway, which is coordinated but not fully dependent on NRF2 signaling [74].

To maintain the natural defense and quality control of the body, healthy stromal cells, including fibroblasts, play a major role in regulating epithelial malignancies. PC-3 and LNCaP prostate cancer cell growth was also shown to be inhibited by conditioned media from healthy human gingival fibroblast cells [75]. We have previously

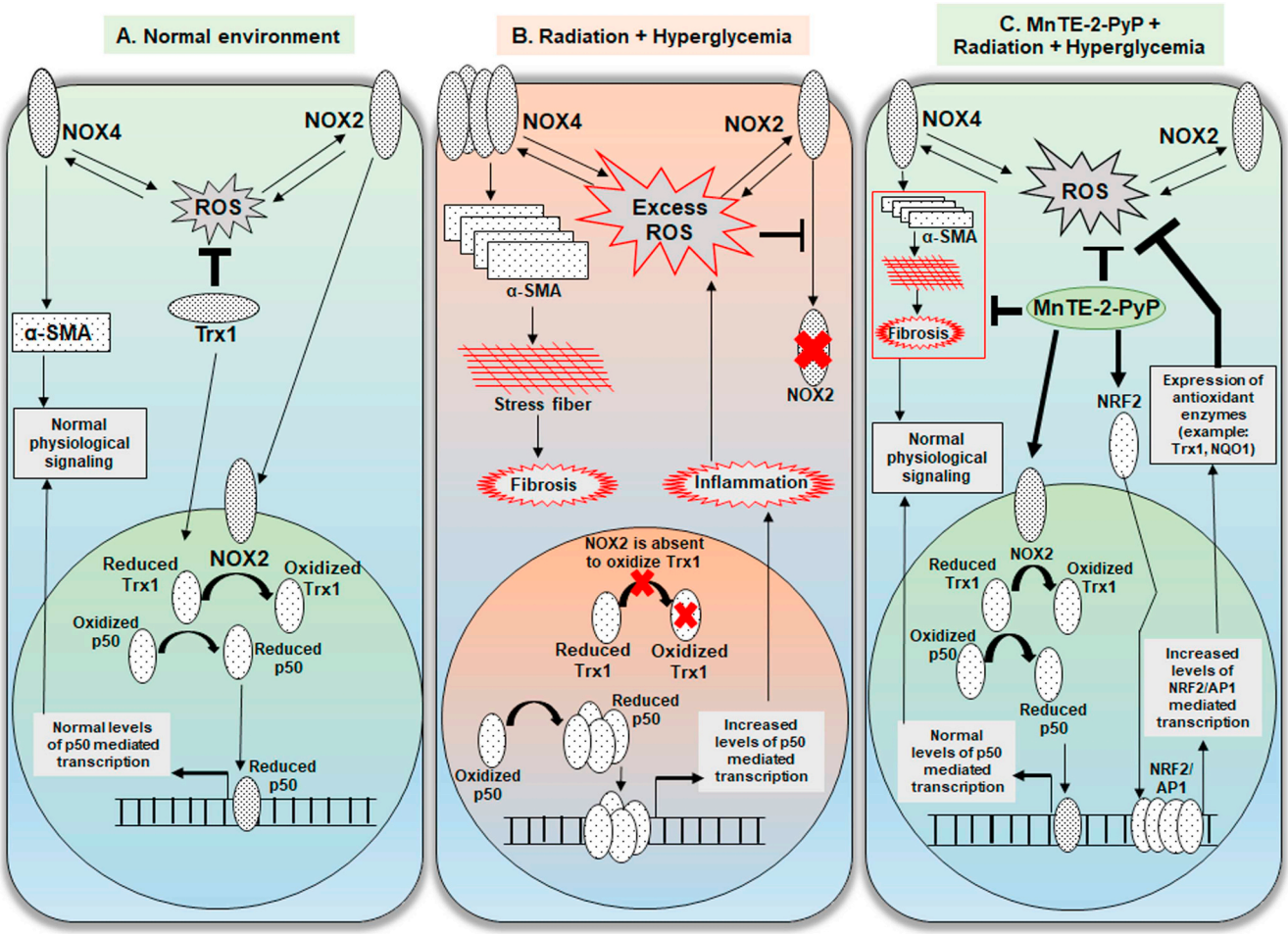


**Fig. 8. Graphical summary of MnTE-2-PyP mediated normal prostate fibroblast protection mechanism. A.** In the normal cellular environment, a basal physiological level of ROS is produced by NOX4 and NOX2 by a positive feedback loop. NOX4 expression positively regulates the expression α-SMA, which maintains the normal levels of cellular elasticity. Two redox modulators, NOX2 and Trx1 translocate to nucleus. NOX2 oxidizes Trx1 that limits the availability of reduced Trx1 in the nucleus to reduce p50 subunit of NFκB. Reduced p50 binds to DNA to maintain NFκB-p50 mediated normal survival response. **B.** In an irradiated and hyperglycemic cellular environment, excess levels of ROS produces increased levels of NOX4 followed by increased levels of α-SMA, which induces pro-fibrotic signaling and accumulates stress fibers in the cell that results in fibrosis. Excess levels of ROS inhibits nuclear localization of NOX2. Absence of NOX2 in the nucleus allows Trx1 mediated increased reduction of p50 and increased DNA binding. This results in an increased inflammatory response in the cell. **C.** In the irradiated and hyperglycemic cellular environment, MnTE-2-PyP directly reduces ROS and also promotes nuclear translocation of NOX2. Nuclear NOX2 inhibits p50 DNA binding by limiting its reduction by Trx1. MnTE-2-PyP increases expression of NRF2 and transcriptional activity of NRF2/AP1. NRF2/AP1 mediated increased expression of antioxidant enzymes inhibit the excess ROS load in the cell.

reported that in an *in vivo* orthotopic prostate tumor model, in presence of radiation, MnTE-2-PyP decreases tumor size and increases survival of the mice [25]. We hypothesized that in a diabetic environment, radiation causes an alteration in stromal cells, which significantly promote tumor growth and recurrence after radiation. MnTE-2-PyP treatment in this situation can maintain the health of normal stromal cells and protect against malignant epithelial cell growth. To study this hypothesis, we have treated PC-3 and LNCaP cells with conditioned media from human normal prostate fibroblasts. PC-3 represents a late endocrine type of prostate tumor growth. Our study revealed that for PC-3 cells, conditioned media from both normo-glycemic and hyperglycemic irradiated fibroblasts, treated with MnTE-2-PyP, caused a significant amount of cell death. LNCaP, a more radiation sensitive cell, represents an early stage of prostate tumor growth. In the case of LNCaP cells, conditioned media from all hyperglycemic conditions (high glucose and radiation + high glucose) caused significant cell death, which was further significantly increased by MnTE-2-PyP treatment. It is reported that, hyperglycemia decreases initial androgen dependent prostate cancer growth like LNCaP cells [76], but enhances the growth and metastatic properties of advanced androgen independent prostate cancer growth like PC3 cells [77]. In our current study, we have also observed a similar effect of hyperglycemia directly on PC-3 and LNCaP cells. Therefore, we are inferring that, in initial androgen dependent prostate cancer growth like LNCaP cells, radiation and hyperglycemia causes significant cancer cell death. MnTE-2-PyP did not show any significant effect directly on PC-3 or LNCaP cells in any of the hyperglycemic conditions. However, MnTE-2-PyP treated fibroblast conditioned media significantly increased LNCaP and PC-3 cell death in irradiated hyperglycemic conditions. Therefore, MnTE-2-PyP treated fibroblasts in the tumor microenvironment have an antitumor effect in the irradiated hyperglycemic environment.

A limitation to this study is that the effect of radiation in a hyperglycemic environment was investigated in P3158 cells only. Although, we have shown that the P3158 cell line behaves similarly to mouse primary prostate cells and human primary prostate fibroblasts [23,59], investigation on these mechanisms in other cell lines should be conducted to confirm the results of this study.

Proper control of metabolism is advantageous for protection against radiation toxicity. Metformin is well reported to effectively regulate the metabolic pathways in diabetics and MnTE-2-PyP can also control

metabolic pathways altered by diabetes [78]. Therefore, we can surmise from this study that the combination of metformin with MnTE-2-PyP, during radiation, may produce even more advantages in a hyperglycemic environment. These experiments will be the focus of future studies.

In conclusion, from this study we can highlight that, although it is known that there is an increased risk of radiation toxicity among diabetics and that diabetic prostate tumors are more resistant to treatment, radiation is still used to treat cancers in diabetics. Besides controlling hyperglycemia, there is also a need to protect the normal tissues from elevated irradiation damage in diabetics. There are no effective therapeutics used for diabetic individuals to reduce normal tissue injury caused by radiation. Therefore, introducing a therapeutic molecule that can help to control hyperglycemia and radiation-induced normal tissue damage, without affecting the antitumor effect of radiation therapy, would be extremely advantageous for diabetic cancer patients receiving radiation therapy. Our data suggests that MnTE-2-PyP protects normal cells from hyperglycemia and radiation by scavenging superoxide, decreasing NF-κB p50 mediated inflammation, and increasing NRF2 mediated antioxidant defense (Fig. 8).

## Declaration of competing interest

There are no conflicts of interest for the authors except Dr. Rebecca E. Oberley-Deegan. Dr. Oberley-Deegan is a consultant with BioMimetix Pharmaceutical, Inc. and holds equities in BioMimetix Pharmaceutical, Inc.

## Acknowledgements

This research is funded by the National Institutes of Health Grants 1R01CA178888, SP20 GM103480 COBRE and Fred and Pamela Buffet Cancer Center Support Grant P30CA036727 to Dr. Oberley-Deegan.

## Appendix A. Supplementary data

Supplementary data to this article can be found online at https://doi.org/10.1016/j.redox.2020.101542.

## References

[1] B.B. Barone, et al., Long-term all-cause mortality in cancer patients with preexisting diabetes mellitus: a systematic review and meta-analysis, J. Am. Med. Assoc. 300 (23) (2008) 2754–2764.
[2] B.B. Barone, et al., Postoperative mortality in cancer patients with preexisting diabetes: systematic review and meta-analysis, Diabetes Care 33 (4) (2010) 931–939.
[3] A.V. D'Amico, et al., Causes of death in men with prevalent diabetes and newly diagnosed high- versus favorable-risk prostate cancer, Int. J. Radiat. Oncol. Biol. Phys. 77 (5) (2010) 1329–1337.
[4] J. Lee, E. Giovannucci, J.Y. Jeon, Diabetes and mortality in patients with prostate cancer: a meta-analysis, SpringerPlus 5 (1) (2016) 1548.
[5] X. Li, et al., Hyperglycaemia-induced miR-301a promotes cell proliferation by repressing p21 and Smad4 in prostate cancer, Canc. Lett. 418 (2018) 211–220.
[6] S.Z. Lutz, et al., Androgen receptor overexpression in prostate cancer in type 2 diabetes, Mol Metab 8 (2018) 158–166.
[7] S.Z. Lutz, et al., Higher prevalence of lymph node metastasis in prostate cancer in patients with diabetes, Endocr. Relat. Canc. 25 (3) (2018) L19–L22.
[8] A. Alashkham, et al., What is the impact of diabetes mellitus on radiation induced acute proctitis after radical radiotherapy for adenocarcinoma prostate? A prospective longitudinal study, Clin Transl Radiat Oncol 14 (2019) 59–63.
[9] D.M. Herold, A.L. Hanlon, G.E. Hanks, Diabetes mellitus: a predictor for late radiation morbidity, Int. J. Radiat. Oncol. Biol. Phys. 43 (3) (1999) 475–479.
[10] C.F. Snyder, et al., Does pre-existing diabetes affect prostate cancer prognosis? A systematic review, Prostate Cancer Prostatic Dis. 13 (1) (2010) 58–64.
[11] N.G. Zaorsky, et al., Prostate cancer patients with unmanaged diabetes or receiving insulin experience inferior outcomes and toxicities after treatment with radiation therapy, Clin. Genitourin. Canc. 15 (2) (2017) 326–335 e3.
[12] M. Koritzinsky, Metformin: a novel biological modifier of tumor response to radiation therapy, Int. J. Radiat. Oncol. Biol. Phys. 93 (2) (2015) 454–464.
[13] M. Rao, et al., Effects of metformin treatment on radiotherapy efficacy in patients with cancer and diabetes: a systematic review and meta-analysis, Canc. Manag. Res. 10 (2018) 4881–4890.
[14] N.A.B. Samsuri, M. Leech, L. Marignol, Metformin and Improved Treatment Outcomes in Radiation Therapy - A Review, vol. 55, Cancer Treat Rev, 2017, pp. 150–162.
[15] K.M. Biernacka, et al., Hyperglycaemia-induced resistance to Docetaxel is negated by metformin: a role for IGFBP-2, Endocr. Relat. Canc. 24 (1) (2017) 17–30.
[16] J.L. Edwards, et al., Diabetes regulates mitochondrial biogenesis and fission in mouse neurons, Diabetologia 53 (1) (2010) 160–169.
[17] J. Liu, et al., Targeting mitochondrial biogenesis for preventing and treating insulin resistance in diabetes and obesity: hope from natural mitochondrial nutrients, Adv. Drug Deliv. Rev. 61 (14) (2009) 1343–1352.
[18] I.C. West, Radicals and oxidative stress in diabetes, Diabet. Med. 17 (3) (2000) 171–180.
[19] S.P. Wolff, Diabetes mellitus and free radicals. Free radicals, transition metals and oxidative stress in the aetiology of diabetes mellitus and complications, Br. Med. Bull. 49 (3) (1993) 642–652.
[20] A. Chatterjee, E.A. Kosmacek, R.E. Oberley-Deegan, MnTE-2-PyP treatment, or NOX4 inhibition, protects against radiation-induced damage in mouse primary prostate fibroblasts by inhibiting the TGF-beta 1 signaling pathway, Radiat. Res. 187 (3) (2017) 367–381.
[21] E.A. Kosmacek, et al., MnTnBuOE-2-PyP protects normal colorectal fibroblasts from radiation damage and simultaneously enhances radio/chemotherapeutic killing of colorectal cancer cells, Oncotarget 7 (23) (2016) 34532–34545.
[22] R.E. Oberley-Deegan, et al., The antioxidant, MnTE-2-PyP, prevents side-effects incurred by prostate cancer irradiation, PloS One 7 (9) (2012) e44178.
[23] S. Shrishrimal, et al., The SOD mimic, MnTE-2-PyP, protects from chronic fibrosis and inflammation in irradiated normal pelvic tissues, Antioxidants 6 (4) (2017).
[24] I. Batinic-Haberle, et al., Design of Mn porphyrins for treating oxidative stress injuries and their redox-based regulation of cellular transcriptional activities, Amino Acids 42 (1) (2012) 95–113.
[25] A. Chatterjee, et al., The addition of manganese porphyrins during radiation inhibits prostate cancer growth and simultaneously protects normal prostate tissue from radiation damage, Antioxidants 7 (1) (2018).
[26] R.E. Oberley-Deegan, et al., The antioxidant mimetic, MnTE-2-PyP, reduces intracellular growth of Mycobacterium abscessus, Am. J. Respir. Cell Mol. Biol. 41 (2) (2009) 170–178.
[27] H.M. Tse, M.J. Milton, J.D. Piganelli, Mechanistic analysis of the immunomodulatory effects of a catalytic antioxidant on antigen-presenting cells: implication for their use in targeting oxidation-reduction reactions in innate immunity, Free Radic. Biol. Med. 36 (2) (2004) 233–247.
[28] G.M. Coudriet, et al., Treatment with a catalytic superoxide dismutase (SOD) mimetic improves liver steatosis, insulin sensitivity, and inflammation in obesity-induced type 2 diabetes, Antioxidants 6 (4) (2017).
[29] G.T. Berry, et al., The effect of glucose and galactose toxicity on myo-inositol transport and metabolism in human skin fibroblasts in culture, Pediatr. Res. 35 (2) (1994) 141–147.
[30] P. Buranasin, et al., High glucose-induced oxidative stress impairs proliferation and migration of human gingival fibroblasts, PloS One 13 (8) (2018) e0201855.
[31] D.C. Han, et al., High glucose stimulates proliferation and collagen type I synthesis in renal cortical fibroblasts: mediation by autocrine activation of TGF-beta, J. Am. Soc. Nephrol. 10 (9) (1999) 1891–1899.
[32] L. Pang, et al., Transcriptomic study of highglucose effects on human skin fibroblast cells, Mol. Med. Rep. 13 (3) (2016) 2627–2634.
[33] Y.H. Xuan, et al., High-glucose inhibits human fibroblast cell migration in wound healing via repression of bFGF-regulating JNK phosphorylation, PloS One 9 (9) (2014) e108182.
[34] A. Martin-Garrido, et al., NADPH oxidase 4 mediates TGF-beta-induced smooth muscle alpha-actin via p38MAPK and serum response factor, Free Radic. Biol. Med. 50 (2) (2011) 354–362.
[35] L.R. Villegas, et al., Superoxide dismutase mimetic, MnTE-2-PyP, attenuates chronic hypoxia-induced pulmonary hypertension, pulmonary vascular remodeling, and activation of the NALP3 inflammasome, Antioxidants Redox Signal. 18 (14) (2013) 1753–1764.
[36] J.R. Matthews, et al., Thioredoxin regulates the DNA binding activity of NF-kappa B by reduction of a disulphide bond involving cysteine 62, Nucleic Acids Res. 20 (15) (1992) 3821–3830.
[37] S.C. Trevelin, et al., Apocynin and Nox2 regulate NF-kappaB by modifying thioredoxin-1 redox-state, Sci. Rep. 6 (2016) 34581.
[38] M.C. Jaramillo, et al., Manganese porphyrin, MnTE-2-PyP5+, Acts as a pro-oxidant to potentiate glucocorticoid-induced apoptosis in lymphoma cells, Free Radic. Biol. Med. 52 (8) (2012) 1272–1284.
[39] S. Nair, et al., Regulation of Nrf2- and AP-1-mediated gene expression by epigallocatechin-3-gallate and sulforaphane in prostate of Nrf2-knockout or C57BL/6J mice and PC-3 AP-1 human prostate cancer cells, Acta Pharmacol. Sin. 31 (9) (2010) 1223–1240.
[40] F.X. Soriano, et al., Transcriptional regulation of the AP-1 and Nrf2 target gene sulfiredoxin, Mol. Cell. 27 (3) (2009) 279–282.
[41] K. Ishii, et al., Role of stromal paracrine signals in proliferative diseases of the aging human prostate, J. Clin. Med. 7 (4) (2018).
[42] T.V. Fiorentino, et al., Hyperglycemia-induced oxidative stress and its role in diabetes mellitus related cardiovascular diseases, Curr. Pharmaceut. Des. 19 (32) (2013) 5695–5703.
[43] P.C. Schulze, et al., Hyperglycemia promotes oxidative stress through inhibition of thioredoxin function by thioredoxin-interacting protein, J. Biol. Chem. 279 (29) (2004) 30369–30374.
[44] K. Nowotny, et al., Advanced glycation end products and oxidative stress in type 2 diabetes mellitus, Biomolecules 5 (1) (2015) 194–222.

[45] A.L. Tan, J.M. Forbes, M.E. Cooper, AGE, RAGE, and ROS in diabetic nephropathy, Semin. Nephrol. 27 (2) (2007) 130–143.
[46] V. Thallas-Bonke, et al., Inhibition of NADPH oxidase prevents advanced glycation end product-mediated damage in diabetic nephropathy through a protein kinase C-alpha-dependent pathway, Diabetes 57 (2) (2008) 460–469.
[47] L.C. Whitmore, et al., NOX2 protects against prolonged inflammation, lung injury, and mortality following systemic insults, J Innate Immun 5 (6) (2013) 565–580.
[48] G. Zhou, et al., Optimal ROS signaling is critical for nuclear reprogramming, Cell Rep. 15 (5) (2016) 919–925.
[49] K.L. Singel, B.H. Segal, NOX2-dependent regulation of inflammation, Clin. Sci. (Lond.) 130 (7) (2016) 479–490.
[50] G. Gloire, J. Piette, Redox regulation of nuclear post-translational modifications during NF-kappaB activation, Antioxidants Redox Signal. 11 (9) (2009) 2209–2222.
[51] M.B. Toledano, et al., N-terminal DNA-binding domains contribute to differential DNA-binding specificities of NF-kappa B p50 and p65, Mol. Cell Biol. 13 (2) (1993) 852–860.
[52] R. Bottino, et al., Response of human islets to isolation stress and the effect of antioxidant treatment, Diabetes 53 (10) (2004) 2559–2568.
[53] P. Joseph, et al., Role of NAD(P)H:quinone oxidoreductase 1 (DT diaphorase) in protection against quinone toxicity, Biochem. Pharmacol. 60 (2) (2000) 207–214.
[54] S.R. McSweeney, E. Warabi, R.C. Siow, Nrf2 as an endothelial mechanosensitive transcription factor: going with the flow, Hypertension 67 (1) (2016) 20–29.
[55] T. Abebe, et al., Nrf2/antioxidant pathway mediates beta cell self-repair after damage by high-fat diet-induced oxidative stress, JCI Insight 2 (24) (2017).
[56] J.A. David, et al., The nrf2/keap1/ARE pathway and oxidative stress as a therapeutic target in type II diabetes mellitus, J Diabetes Res 2017 (2017) 4826724.
[57] A.T. Dinkova-Kostova, A.Y. Abramov, The emerging role of Nrf2 in mitochondrial function, Free Radic. Biol. Med. 88 (Pt B) (2015) 179–188.
[58] Y. Zhao, et al., Resveratrol attenuates testicular apoptosis in type 1 diabetic mice: role of Akt-mediated Nrf2 activation and p62-dependent Keap1 degradation, Redox Biol 14 (2018) 609–617.
[59] S. Shrishrimal, et al., Manganese porphyrin, MnTE-2-PyP, treatment protects the prostate from radiation-induced fibrosis (RIF) by activating the NRF2 signaling pathway and enhancing SOD2 and sirtuin activity, Free Radic. Biol. Med. 152 (2020) 255–270.
[60] Y. Zhao, et al., A novel redox regulator, MnTnBuOE-2-PyP(5+), enhances normal hematopoietic stem/progenitor cell function, Redox Biol 12 (2017) 129–138.
[61] Z. Sun, Y.E. Chin, D.D. Zhang, Acetylation of Nrf2 by p300/CBP augments promoter-specific DNA binding of Nrf2 during the antioxidant response, Mol. Cell Biol. 29 (10) (2009) 2658–2672.
[62] P. Nioi, et al., The carboxy-terminal Neh3 domain of Nrf2 is required for transcriptional activation, Mol. Cell Biol. 25 (24) (2005) 10895–10906.
[63] H. Pan, et al., SIRT6 safeguards human mesenchymal stem cells from oxidative stress by coactivating NRF2, Cell Res. 26 (2) (2016) 190–205.
[64] J. Zhang, et al., BRG1 interacts with Nrf2 to selectively mediate HO-1 induction in response to oxidative stress, Mol. Cell Biol. 26 (21) (2006) 7942–7952.
[65] J.M. Lee, J.A. Johnson, An important role of Nrf2-ARE pathway in the cellular defense mechanism, J. Biochem. Mol. Biol. 37 (2) (2004) 139–143.
[66] T. Xie, et al., ARE- and TRE-mediated regulation of gene expression. Response to xenobiotics and antioxidants, J. Biol. Chem. 270 (12) (1995) 6894–6900.
[67] K. Hirota, et al., AP-1 transcriptional activity is regulated by a direct association between thioredoxin and Ref-1, Proc. Natl. Acad. Sci. U. S. A. 94 (8) (1997) 3633–3638.
[68] S.J. Wei, et al., Thioredoxin nuclear translocation and interaction with redox factor-1 activates the activator protein-1 transcription factor in response to ionizing radiation, Canc. Res. 60 (23) (2000) 6688–6695.
[69] V. Sueblinvong, et al., Nuclear thioredoxin-1 overexpression attenuates alcohol-mediated Nrf2 signaling and lung fibrosis, Alcohol Clin. Exp. Res. 40 (9) (2016) 1846–1856.
[70] Y. Li, A.K. Jaiswal, Regulation of human NAD(P)H:quinone oxidoreductase gene. Role of AP1 binding site contained within human antioxidant response element, J. Biol. Chem. 268 (28) (1993) 21454.
[71] T. Xie, A.K. Jaiswal, AP-2-mediated regulation of human NAD(P)H: quinone oxidoreductase 1 (NQO1) gene expression, Biochem. Pharmacol. 51 (6) (1996) 771–778.
[72] M. Meyer, R. Schreck, P.A. Baeuerle, H2O2 and antioxidants have opposite effects on activation of NF-kappa B and AP-1 in intact cells: AP-1 as secondary antioxidant-responsive factor, EMBO J. 12 (5) (1993) 2005–2015.
[73] A.A. Belanova, et al., Effects of JUN and NFE2L2 knockdown on oxidative status and NFE2L2/AP-1 targets expression in HeLa cells in basal conditions and upon sublethal hydrogen peroxide treatment, Mol. Biol. Rep. 46 (1) (2019) 27–39.
[74] B.A. Davidson, et al., NADPH oxidase and Nrf2 regulate gastric aspiration-induced inflammation and acute lung injury, J. Immunol. 190 (4) (2013) 1714–1724.
[75] F. Iacopino, C. Angelucci, G. Sica, Interactions between normal human fibroblasts and human prostate cancer cells in a co-culture system, Anticancer Res. 32 (5) (2012) 1579–1588.
[76] A. Barbosa-Desongles, et al., Diabetes protects from prostate cancer by down-regulating androgen receptor: new insights from LNCaP cells and PAC120 mouse model, PloS One 8 (9) (2013) e74179.
[77] Y.L. Huang, et al., High glucose induces VEGF-C expression via the LPA1/3-akt-ROS-LEDGF signaling Axis in human prostate cancer PC-3 cells, Cell. Physiol. Biochem. 50 (2) (2018) 597–611.
[78] M.M. Delmastro-Greenwood, et al., Mn porphyrin regulation of aerobic glycolysis: implications on the activation of diabetogenic immune cells, Antioxidants Redox Signal. 19 (16) (2013) 1902–1915.